DESIGN, SIMULATION AND ANALYSIS OF A NOVEL ROTARY VALVE FOR IMPROVEMENT IN THE EFFICIENCY OF AN INTERNAL COMBUSTION ENGINE

by

Wenbo Dong

A Dissertation Submitted in Partial Fulfillment of the Requirements for the Degree of

Doctor of Philosophy

Middle Tennessee State University

May 2024

Dissertation Committee:

Dr. Vishwas Bedekar, Chair

Dr. Joshua Phillips

Dr. Donglin Wang

Dr. Misa Faezipour

ACKNOWLEDGEMENTS

Dr. Vishwas Bedekar, my academic advisor in COMS PhD program, for his unlimited support and motivation during my research.

Dr. Charles Perry, my mentor for my MS study and life in MTSU during my first year in America, for his teaching, supporting and motivation during my research.

Dr. Joshua Phillips for serving on my dissertation committee.

Dr. Donglin Wang for serving on my dissertation committee and advice during my research.

Dr. Misa Faezipour for serving on my dissertation committee.

Dr. John Wallin, MTSU COMS PhD program director, for his support and continuous help throughout the years.

Mr. Rick Taylor for his machining work support, advice and the patience he gives to his students.

Mr. William Harper, my friend, for his advice and welding technique support.

Dr. Yiting Wang, my friend, for his mathematics support.

Dr. Jingsai Liang, my friend, for his mathematics and MATLAB technique support.

Mr. Justin Roberts, my friend, for his English writing advice.

ABSTRACT

Numerous studies have concentrated on enhancing the efficiency of internal combustion engines through various means, including refined design, superior materials, and regenerative technologies. Toyota recently reported a 40% gasoline engine efficiency with their Prius model in 2016. However, further research is warranted for improvement towards reaching the theoretical value of 73% efficiency as outlined by the Carnot Theorem.

The first section of this dissertation gives an in-depth introduction of internal combustion engine from aspects including the history and the popular modern design as well as the history of the inventions of rotary valve engines.

In the second section, the concept of using rotary valve instead of the conventional poppet valve for internal combustion engine is proposed. The study lists major drawbacks of the conventional poppet valve and explains the advantages of the rotary valve in general. A novel vertical positioned, servo motor driven, bell shape rotary valve is proposed to potentially improve the efficiency of a known conventional valve designed engine. The data of the new design is compared to the conventional poppet valve design with respect to several parameters to discuss its working principle and advantages over the conventional valve mechanism. Modeling is performed using Python programming to predict the valve opening mechanism. The experimental design is setup to control and tune different parameters accordingly within the reasonable range of engine speed viz. 1000-6000 RPM to simulate various working conditions. The maximum opening area for the rotary valve is calculated to be 0.795 sq.in which is smaller than the poppet valve's area of 1.315 sq.in. However, under an example of 2900

RPM, the rotary valve was able to remain fully opened with constant efficiency of about 54% from 40 to 160 degrees of the crankshaft angle, while the poppet valve achieves 88% efficiency at 90 degree of the crankshaft angle and the efficiency significantly drops on either side of the maximum. Calculation shows that the proposed rotary valve can gain better performance with engine speed below 4400 RPM which is acceptable for real world use.

Building on these findings, the third section develops and improves the rotary valve mechanism and the engine design. With key parameters such as displacement, cylinder bore, stroke, and compression ratio remaining the same, a transvers positioned, servo motor driven, spherical shape rotary valve is introduced. Instead of retrofitting the existing engine head with the bell-shaped valve, a new engine head design is developed, aiming to minimize the overall number of components required.

A new spindle port shape is proposed, accompanied by a comparative calculation with the traditional circular shape. The valve flow coefficient prediction and in-cylinder pressure prediction are performed followed by volumetric efficiency prediction.

An engine simulation based on the ideal Otto cycle is conducted with adequate predictions and parameter settings. The results reveal that the spherical shape rotary valve achieves a valve opening area comparable to that of the conventional poppet valve. Additionally, the spindle valve opening port shape delivers a volumetric efficiency gain of up to 3% compared to the circular shape at the same crankshaft angle. This improvement in volumetric efficiency is attributed to the engine's kinematics and mechanical engineering principles. The rapid creation of valve opening area by the rotary

valve during the intake process results in very low negative work, as depicted in the P-V diagram from the engine simulation.

Overall, these findings underscore the potential of the spherical shape rotary valve and spindle valve opening port shape to enhance engine performance and efficiency, offering valuable insights for further advancements in internal combustion engine design.

TABLE OF CONTENTS

LIST OF TABLES

LIST OF FIGURES

CHAPTER 1 INTRODUCTION

1.1 Terminology

The subsequent compilation comprises commonly used terminology in the design of internal combustion engines:

IC engine. An internal combustion engine is a type of heat engine that converts the chemical energy stored in fuel into mechanical energy. This process occurs through the combustion of a fuel-air mixture within the engine's combustion chamber. The engine typically consists of a series of cylinders in which pistons move up and down. The combustion process forces these pistons to reciprocate, and their motion is then converted into rotational motion through a crankshaft. Internal combustion engines (reciprocating engines only) are widely used in various applications, including automobiles, motorcycles, aircraft, boats, and power generators, due to their efficiency and ability to provide a reliable source of mechanical power.

Spark ignited. This refers to a combustion process in internal combustion engines where the ignition of the air-fuel mixture is initiated by an electric spark produced by a spark plug. In spark-ignited engines, such as gasoline engines, the air-fuel mixture is first compressed within the combustion chamber. When the piston reaches the top of its compression stroke, a spark plug generates an electric spark, igniting the compressed mixture.

Top dead center. It is also abbreviated as TDC. TDC refers to the position of a piston within an internal combustion engine when it has reached the highest point in its travel within the cylinder. In the engine's four-stroke cycle, TDC is a specific point in the compression and power strokes.

Bottom dead center. It is also abbreviated as BDC. BDC refers to the position of a piston within an internal combustion engine when it has reached the lowest point in its travel within the cylinder. In the four-stroke cycle of an engine, BDC is a specific point in the exhaust and intake strokes.

Ignition timing. Ignition timing refers to the precise moment in the engine's four-stroke cycle when the spark plug fires to ignite the compressed air-fuel mixture in the combustion chamber. This timing is critical for the efficient and controlled combustion of the fuel, which influences the engine's performance, efficiency, and emissions. The ignition timing is typically expressed in degrees before or after Top Dead Center (TDC), representing the crankshaft's position in the engine cycle. Advancing or retarding the ignition timing can have a significant impact on engine behavior.

Crankshaft angle. This refers to the angular position of the crankshaft in an internal combustion engine, measured in degrees of rotation. The crankshaft is a key component responsible for converting reciprocating motion (up-and-down movement of the pistons) into rotational motion, which drives the vehicle's transmission and ultimately powers the wheels. The crankshaft angle is typically measured in relation to a reference point, often Top Dead Center (TDC) or Bottom Dead Center (BDC). The entire engine cycle, completing one revolution of the crankshaft, covers 360 degrees. The crankshaft angle is crucial for determining the timing of various events in the engine, such as the opening and closing of valves and the ignition timing.

Valve opening. This refers to the moment the intake or exhaust valve begins to move from a closed to an open position. In an internal combustion engine, the opening of valves is crucial for controlling the flow of air and exhaust gases in and out of the

combustion chamber. During the intake stroke, the intake valve opens to allow the air-fuel mixture into the cylinder. In the exhaust stroke, the exhaust valve opens to enable the expulsion of burned gases from the cylinder. The precise timing of valve opening is a critical factor in engine performance, and it is often determined by the engine's design specifications, including the camshaft profile and timing.

Valve closing. This refers to the moment the intake or exhaust valve begins to move from an open to a closed position. During the intake stroke, the intake valve closes to seal the combustion chamber and facilitate the compression of the air-fuel mixture. In the exhaust stroke, the exhaust valve closes to prevent any further escape of gases and allow the piston to compress the remaining exhaust gases. The precise timing of valve closing is a critical factor in engine performance, and it is often determined by the engine's design specifications, including the camshaft profile and timing.

Compression ratio. Compression Ratio is a fundamental parameter in internal combustion engines and is defined as the ratio of the total cylinder volume at the BDC to the volume at TDC. It is typically expressed as a numerical ratio, such as 10:1, representing the ratio of the larger cylinder volume to the smaller volume. A higher compression ratio indicates that the air-fuel mixture is compressed to a smaller volume before ignition, leading to more efficient combustion and potentially greater power output. However, excessively high compression ratios can lead to issues like pre-ignition.

Volumetric efficiency. Volumetric efficiency is a measure of how well an internal combustion engine utilizes the available air intake volume during its operation. It is expressed as a percentage and represents the ratio of the amount of air an engine can draw into the cylinders during the intake stroke to the total cylinder volume.

Mathematically, volumetric efficiency is calculated by the ratio of the actual intake volume and the maximum cylinder volume.

In an ideal scenario, where the engine fills its cylinders completely with air during each intake stroke, the volumetric efficiency would be 100%. However, various factors, such as restrictions in the air intake system, valve timing, and design considerations, can impact the engine's ability to achieve complete cylinder filling. Therefore, volumetric efficiency is often less than 100%, and engine designers and tuners work to optimize it for improved performance and efficiency.

Valve overlap. This is a term used in the context of internal combustion engines and refers to the period when both the intake and exhaust valves are briefly open at the same time. This occurs during the transition between the exhaust stroke and the intake stroke. During the exhaust stroke, the exhaust valve opens to allow the burned gases to exit the combustion chamber. Simultaneously, as the piston approaches the end of the exhaust stroke, the intake valve starts to open to allow fresh air and fuel to enter the chamber for the upcoming intake stroke.

Valve overlap is typically expressed in degrees of crankshaft rotation. A certain degree of overlap is often intentional in engine design, and it can influence engine performance characteristics. The benefits of valve overlap include improved scavenging. However, excessive overlap can lead to negative effects, such as decreased idle quality and increased emissions. [1]

1.2 Internal Combustion Engine

Instead of powering a transmission through the crankshaft with repeating combustion, the origins of the internal combustion engine were utilizing combustion to

lift a giant weight, dating back to the Renaissance.[2] The concept involved igniting fuel within a vertically situated cylinder, causing the combustion to propel a piston upward. Subsequently, the atmospheric pressure drew the piston back as the explosive gases cooled.[3] The recognizable internal combustion used in automobiles today emerged in 1876 with Otto's introduction of the spark-ignition engine, followed by Diesel's creation of the compression-ignition engine in 1892.[4] Since then, ongoing research in the operation of internal combustion engines has led to the development of various designs aimed at experimentally enhancing performance, efficiency, and reliability.

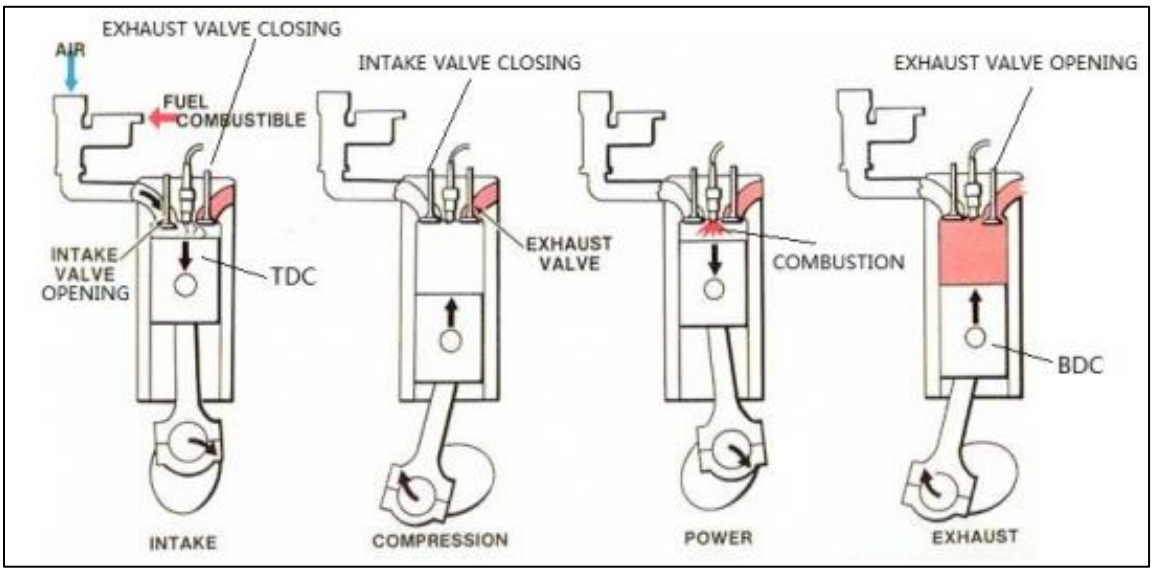

Figure 1: Four-Stroke Reciprocating Internal Combustion Engine Operation

The reciprocating internal combustion engine stands as one of the most prevalent sources of mechanical power in the contemporary world. While there exist diverse designs for reciprocating internal combustion engines, the focus in this work centers on the four-stroke spark ignition engine cycle.

1.1.1 Fundamental Principles

Figure 1 illustrates a diagrammatic representation of a four-stroke reciprocating internal combustion engine operation. The described engine employs a crankshaft and connecting rod to produce a reciprocating motion in the piston. The motion creates compression and then is driven by the expansion of the gas above the piston within the combustion chamber. The cylinder head features both inlet and exhaust valves, facilitating the exchange of gas, along with a spark plug for igniting the charge.

The term "four-stroke cycle" derives from the four primary processes executed by the engine. During the intake stroke, the engine initiates at Top Dead Center (TDC), representing the highest point the piston can reach, and the intake valve opening allows the aspiration of the air/fuel mixture into the cylinder. Following the intake stroke, the intake valve closes, and the piston moves past Bottom Dead Center (BDC), ascending to compress the mixture. After the compression stroke, ignition occurs—either through a spark plug (in gasoline engines) or compression heat (in diesel engines)—when the piston is at TDC. The resultant expansion of the combustion gases propels the piston downward during the expansion stroke. Eventually, the piston passes BDC, and ascends, and the exhaust valve opening facilitates the release of exhaust gases.

1.1.2 Modern poppet valve engine

The design of poppet valve engines has undergone substantial evolution since the early stages of the internal combustion engine. Many factors have been considered and modified to obtain different objectives based on various design requirements. In terms of combustion chamber geometry, after trailing through a “bathtub” shape with a flathead engine [5, 6], “wedge” shape [7, 8], and “pent-roof” shape [9-11], it is commonly

accepted that researchers have reached a consensus that “pent-roof” shape combustion chamber is more suitable for modern high-performance applications. Similarly, piston top shape also has variations including flat-top, dome, and dish that fit in their specific supplications based on different requirements for the compression ratio and valve clearance. [12-14] Modern internal combustion engines usually feature four valves with two intake valves and two exhaust valves. [4]

1.3 Rotary valve engine

Rotary valve engines represent a distinct and innovative category within the realm of internal combustion engines. Unlike traditional poppet valve designs, rotary valve engines utilize a rotating mechanism for gas intake and exhaust. This unique approach brings several advantages, impacting efficiency, performance, and engine design. At the core of a rotary valve engine lies the rotary valve mechanism, a departure from the conventional reciprocating poppet valves. This mechanism typically consists of a rotating assembly that controls the intake and exhaust phases of the engine cycle. Unlike the linear motion of poppet valves, the rotary valve's rotational movement streamlines gas flow, reducing turbulence and optimizing combustion efficiency [15-18]. More advantages of a rotary valve over a conventional poppet valve have been reported in research [19-21].

The rotary valve's continuous rotation facilitates smoother gas intake and exhaust, minimizing flow restrictions and enhancing overall efficiency. A rotary valve can have a larger opening area in an equivalent occupied space as a poppet valve. Optimized combustion chambers can be designed using a rotary valve that will provide a high discharge coefficient maximizing the airflow in the combustion chamber. Rotary valve

engines often boast a more compact design compared to their poppet valve counterparts, allowing for a higher power-to-weight ratio. Fewer moving parts in rotary valve design would result in reduced costs of manufacturing and maintenance. Elimination of reciprocating valve motion can result in reducing frictional power losses of the engine. The rotary valve's rotational motion reduces friction compared to the reciprocating motion of poppet valves, contributing to increased engine longevity. The rotary valve mechanism allows for precise control over the timing of gas intake and exhaust, optimizing combustion and power delivery.

1.4 History of rotary valve

The history of rotary valve engines dates back to the early 19th century when various inventors and engineers experimented with alternative valve mechanisms. One notable pioneer was The Crossley Brothers, a prominent British engineering company, that played a role in the historical development of rotary valve engines. They were known for their contributions to various types of engines, including the production of horizontal gas engines in the late 19th and early 20th centuries. The Crossley Brothers were among the pioneers and experimented with alternative valve mechanisms, exploring the potential advantages of rotary valve designs [22]. Figure 2 shows the inside of the Crossley rotary valve.

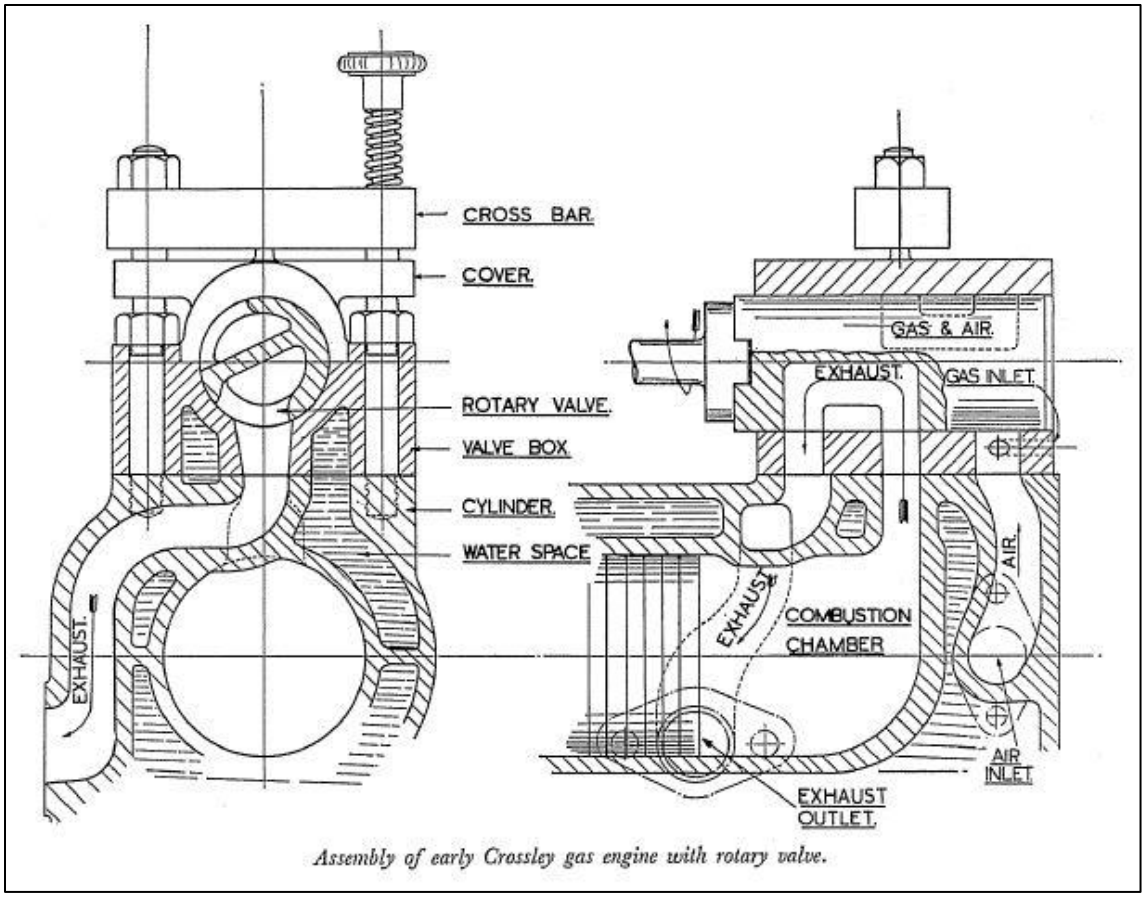

Figure 2: Crossley Rotary Valve

The true rotary valve engine concept gained traction in the mid-20th century, notably with the development of the Norton Rotary, a motorcycle engine introduced by the British manufacturer Norton in the 1950s. They introduced the Manx engine originated from a square-500 design, featuring a unique configuration. Its distinctive element was a cylindrical valve positioned at the top, actuated by bevel gears connected to a vertical shaft. This vertical shaft, in turn, was driven by another vertical shaft through two small pinions. The power transfer continues as the second vertical shaft was linked to the crankshaft through bevel gears. This intricate arrangement of components highlighted the innovative engineering behind the Manx engine, showcasing a well-coordinated

system of interconnected mechanisms [23]. Figure 3 shows the structure of the Manx rotary valve engine.

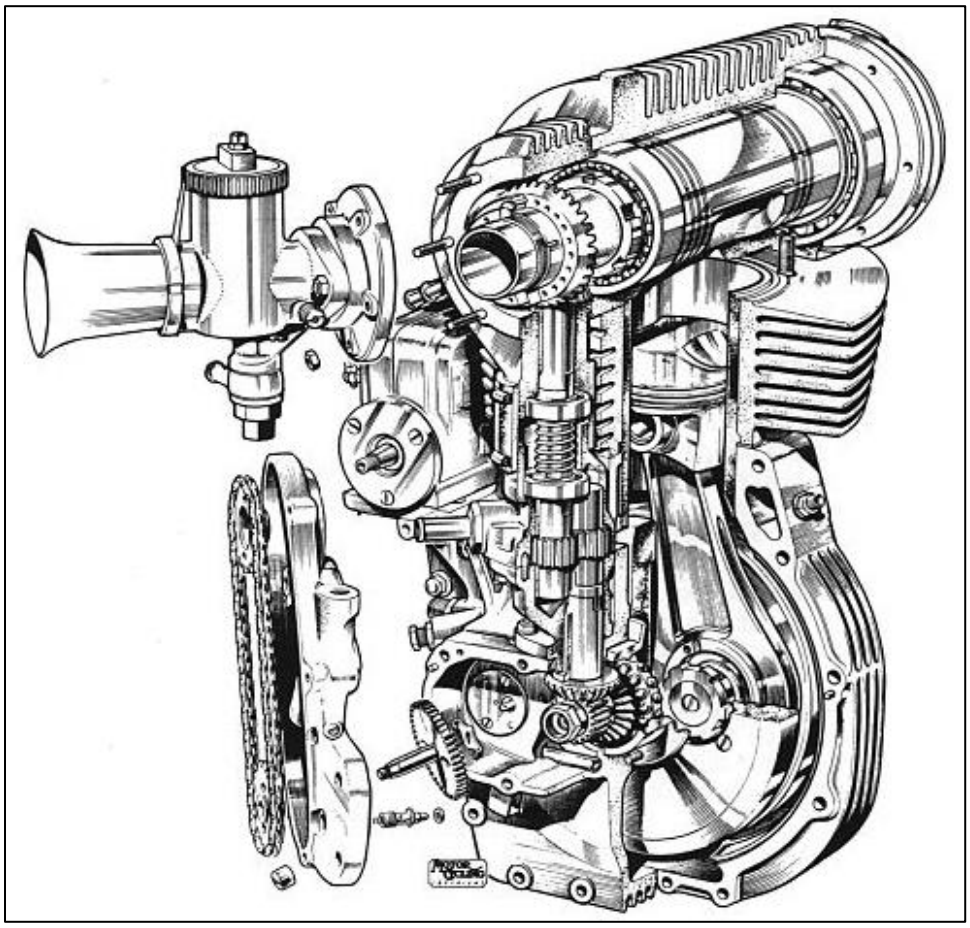

Figure 3: Manx Rotary Valve Engine

While the above shows the typical constructions of the horizontal rotary valve, there have been vertical oriented rotary valve designs throughout the years.

The Peacey valve featured a vertical rotor with a funnel shape, incorporating cut-out segments to function as valve ports. This design shared certain characteristics with the subsequently developed Aspin rotary valve. The valve was installed on a Blackburne engine, where oil was supplied from the oil pump to the rotating valve spindle. The

spindle, equipped with a spiral groove on its lower section, facilitated the pumping of oil downward between the valve cone and the cylinder head. To safeguard against oil loss, the valve gear and its drivetrain were entirely enclosed [24]. Figure 4 shows the design of the Peacey rotary valve.

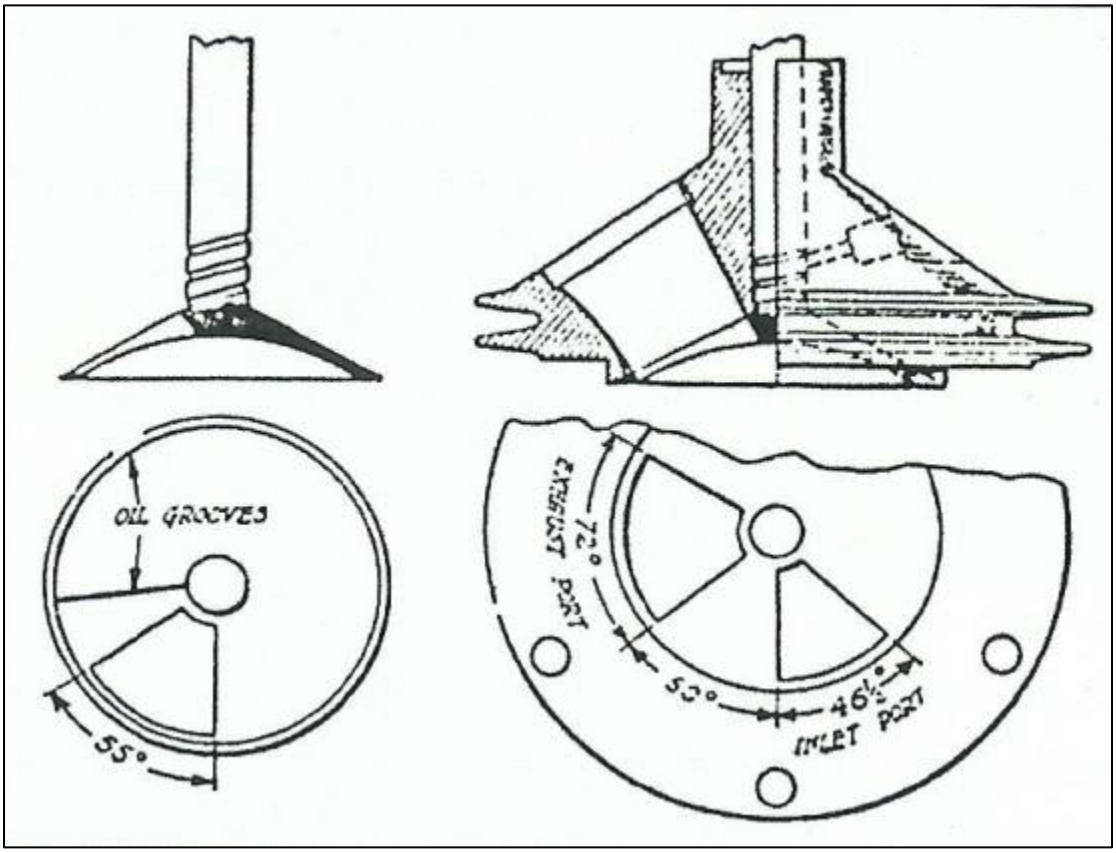

Figure 4: Peacey Rotary Valve

The Aspin valve comprises a cone-shaped metal component installed on the cylinder head in internal combustion engines. Patented by Frank Metcalf Aspin in 1939, although the concept predates this period. The valve's rotation facilitates the essential opening and closing actions for intake and exhaust. Connected to the engine perpendicularly to the cylinder block via a shaft at its apex, this configuration permits horizontal rotation above the cylinder when activated. Hollow in structure, the valve

features a significant cut-out on one side. This design allows gases to alternately enter the combustion chamber and exit to the exhaust system by aligning holes in the valve shaft with cylinder-head ports, facilitating the passage of gases [25]. Figure 5 shows the Aspin valve structure.

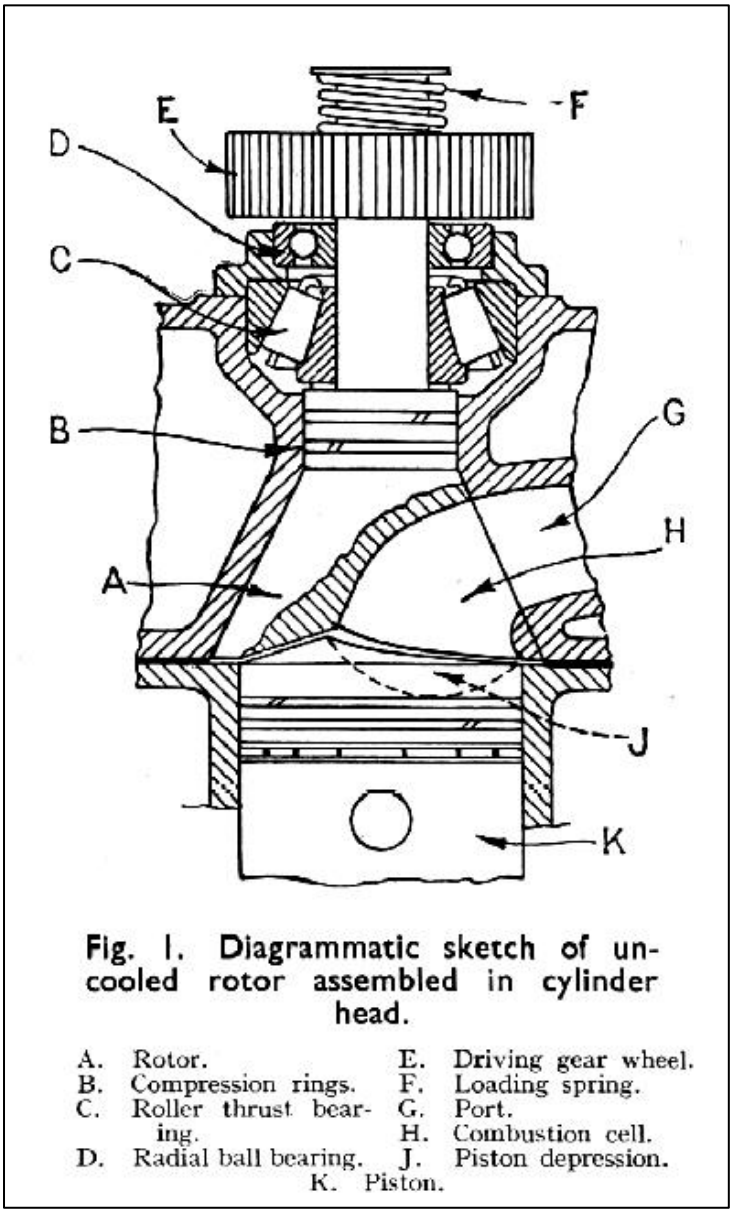

Fig. 1. Diagrammatic sketch of uncooled rotor assembled in cylinder head.

A. Rotor.
B. Compression rings.
C. Roller thrust bearing.
D. Radial ball bearing.
E. Driving gear wheel.
F. Loading spring.
G. Port.
H. Combustion cell.
J. Piston depression.
K. Piston.

Figure 5: Aspin Rotary Valve

Throughout the latter half of the 20th century and into the 21st century, interest in rotary valve engines persisted, with sporadic research and development efforts. Ongoing advancements in materials, engineering, and a growing emphasis on environmental considerations spark renewed interest and further development in the future.

1.5 Method of research

The study commences with comprehensive reviews, including a mass survey aimed at understanding the historical evolution and contemporary trends of internal combustion engines. Through this survey, a brief overview of the principles underlying both conventional poppet valve and rotary valve systems is formed. In this research, a variety of software tools are employed to aid in visualizing and simulating the designs, facilitating a deeper exploration of their performance characteristics and potential improvements.

To create the 3D drawing and test the dimension and assembly, Siemens NX UG, Autodesk AutoCAD, Fusion 360, and QIDI Print are used.

Later in the calculation process, majority of the code is based on Python along with MATLAB. A link to the Python code is provided at the end of this dissertation.

CHAPTER 2 OBJECTIVES OF RESEARCH

The objectives of the research can be divided into a few sections.

- To gain a thorough understanding of internal combustion engines.

Various relevant textbooks and research papers are reviewed to study the principles, constructions, advantages, and disadvantages of different engine designs. Different valve train layouts are studied to learn its history, characteristics, development directions, and performance. The rotary valve systems, specifically, are thoroughly reviewed. The history, properties, different constructions, performance, current development, problems, and future possibilities are discussed.

- To prove the feasibility of using rotary valve for internal combustion engines.

A new rotary valve system is proposed for feasibility analysis to determine the later research direction. In the proposed valve feasibility analysis, the mechanical drawing of the new valve system are presented. The design details of each component are explained and the mathematical analyses are expressed to show the feasibility and the advantages of the new valve system.

- To improve the rotary valve and validate the concept using engine simulation.

Once the feasibility is proven, a further refined and developed rotary valve system is proposed. The mechanical drawing is provided for the improved design showing better layout and performance. The improvements are discussed in detail. An engine simulation is completed along with rotary valve volumetric efficiency prediction.

CHAPTER 3 DESIGN, MODELING AND FEASIBILITY ANALYSIS OF ROTARY VALVE FOR INTERNAL COMBUSTION ENGINE

3.1 Introduction and Literature Review

Recent advancements in the design of internal combustion engines have made lot of progress towards improvement in thermal and mechanical efficiencies of the engine as well as resulting in higher mileage and range of the vehicle. Valve design has evolved over the decades due to the constant demand for highly efficient and high-power automobiles with 6+ cylinders. The valve opening area and timing were some of the most critical parameters to achieve high efficiency. The transverse rotary valve was the most direct conversion to the original piston internal combustion engine due to the structural similarity to the conventional poppet valve configuration. This section demonstrated the research progress that were reported in the literatures, followed by the challenges facing the conventional poppet valve design and the advantages of rotary valve design.

Chow, Watson, and Wallis have done a study about combustion in a high-speed rotary valve spark-ignition engine. In this research, they designed the combustion model that can simulate a combustion performance for a transverse rotary valve engine with up to 18000 revolutions per minute (RPM) of engine speed. The experiment data indicated the paths to engine combustion process improvements. According to their study, engine power output increased with volumetric efficiency and in-cylinder velocity, with respect to RPM, contributed to the engine power output with its increase. [26] Bishop Innovations published their work in 2007 with a dual ports single rotary valve design. In their research, a string of timing gears was applied to replace the timing chain/belt to

transfer the power from the crankshaft to the rotary valve. Integrating both intake and exhaust ports into a single column-shaped valve body, the Bishop rotary valve maximized the port size and occupied most space above the cylinder for gas exchange. The rotational motion removed the inertia from the conventional reciprocating poppet valve. To form a proper seal, similar to a piston ring, a seal was installed around the rotary valve vent and was slightly preloaded to push against the contacting surface. The developer stated a 16 Kg weight reduction with their rotary valve when building a 3-liter V10 F1 engine compared to the engine that has the poppet valve. The research also indicated that performance remained the same with their rotary conversion and the peak volumetric efficiency was the same as well. The dual ports single valve was successful on F1 racing cars from 1995 to 2005 in reaching 20000 to 24000 RPM. [26]

In 2015, Boretti and Scalzo optimized the pneumatic poppet valve. In the study, they also designed a rotary valve that provides ultra-sharp valve opening and closing. According to the research, a rotary valve had the capacity to improve the volumetric efficiency by providing the largest valve area in a short time. Their experiment tried the compression ratio up to 14:1. The achievement of their rotary valve included higher power density, better engine breathing properties, higher fuel conversion efficiency and weight reduction. [27] Boretti's other research also indicated that rotary valves could provide a chance for the engine to gain a higher compression ratio. The study included Bishop Innovations' achievement that solved gas sealing, oil sealing, excessive friction and seizure caused by thermal and mechanical distortion. The research also indicated that the gas flow will be different from the poppet valve engine due to the lack of piston top valve clearance pockets. Muroki, Moriyoshi and Sekizuka published their work in 1999

focusing on the flow dynamic and the friction effect. The study proved that rotary valves can save up to 40 percent on valve-driving mechanical loss. However, the notch profile in the early stage of the intake stroke would affect the intake flow. [18] Muzakkir, Patil and Hirani also conducted a study in 2015 with a hypothesized erect rotary valve that works with a Magneto-Rheological fluid instead of a solid metal valve seat to form a proper seal and prevent wearing out. However, none has fabricated and tested this configuration of the rotary valve. [28]

Brown, Atluri and Schmiedeler introduced a set of floating valve seal systems. In which the spring would push the floating valve seal against the rotary valve to form a seal and self-adjust to accommodate the wearing out. In the study, the rotary valve was fitted to high-speed pneumatic machine. [29] In 2014, Zibani, Chuma and Marumo designed, tested, and implemented a rotary valve control unit for a single-cylinder engine. The study addressed problems of conventional valve engine, such as piston-valve interference and the complexities of the poppet valve train. They proposed a software-operated electronically controlled rotary valve (ECRV) that manages the system and offers fully flexible valve event control. According to the study, the throttle body could be eliminated to reduce pumping loss. Since the engine control unit successfully operated the experimental system, the idea of extending the electronically controlled rotary valve into a multi-cylinder engine was shown feasible. The feature of the electric rotary valve also provided the possibility for variable timing control. [30] An analysis presented by Tsu showed an operation with intake and exhaust valve overlap. He implemented a program based on mathematical modeling to estimate engine performance. The predicted results

fitted mostly well with the experimental data that was collected from three different engine examples. [31]

Theobald, Lequesne and Henry fitted a new programmable electromagnetic valve actuator on a single-cylinder research engine to explore efficiency and emission improvements with variable valve actuation operation. Research only showed a net-efficiency gain under certain conditions. However, the actuator's electrical input energy loss was less than the friction loss for a conventional valvetrain. [32] In 2017, Stone, Kelly, Geddes and Jenkinson fitted an electric motor actuated valve-train on a Jaguar Land Rover 4-cylinder engine and was able to gain up to 7.5 percent of fuel economy improvement. The study also confirmed throttle-less operation feasibility. [33] In 2019, Myers introduced a novel engine head design with a new rotary valve system. The study indicated the new design helps volumetric efficiency and cylinder flow. With the new design, the combustion process took place more evenly and consistently. The disk-shape valve rotor design did not provide any mechanical sealing ability and required two radial seals which mimic the side seals in a Wankel engine. However, the Wankel engine side seal was not an optimum solution on its own. The valve rotors were interconnected hence the limitation in variable valve timing. [34]

Hongyu Mu and the team members published their research in 2022 about improving engine thermal efficiency. According to the experiment, the research engine DAM16N achieved its minimum fuel consumption when the engine was running between 2000-2800 RPM. [35] In 2015, Kopac and Kokturk observed the optimum engine speed. Their study presented both experimental measurements and analytical modeling

throughout a wide range of engine speeds. And 2580 RPM was found to be the best running point for the specific engine. [36]

3.1.1 Benchmark Engine Model

In this research, an engine from a 1996 SUZUKI DR200 motorcycle that features 4-stroke, spark-ignited, timing chain driven dual-overhead-camshaft, gasoline fuel powered is selected as the benchmark that provides the base data for all parameters. The improvements are also developed and compared based on the selected engine structure.

3.1.2 Shortcomings in Conventional Valvetrain

In order to accomplish gas exchange throughout the entire process of combustion, the engine has to have a series of intake and exhaust valve movements based on a timing setup. Conventionally, the valves are driven by the engine crankshaft with a seies of mechanical transition systems. The entire system between the crankshaft and the valve is called the valvetrain. On the mass-produced engines, the valvetrain can be classified into two basic categories which are pushrod driving and belt driving while in the belt driving category, timing belt and timing chain are applied for different demands. There are several challenges identified in the literature for the conventional valvetrain such as inertia, friction, timing and duration. These challenges are explained in detail below. [37]

Valve interference. Based on the operation of a four-stroke engine, the calculation shows that at 4000 revolutions per minute (RPM), a valve opens 2000 times every minute which converts to 33 times a second. Due to the inertia, a heavy valve train keeps its motion further until the valve spring catches it. Eventually, under higher RPM, the valve and its components are struck too far to be caught by the valve spring in time. Valve floating and valve-piston interference occur. [38]

According to Trzesniowski, conventional valve springs are capable of supporting up to 16000 rpm without causing valve floating. However, such a system requires a much complex valve train concept. [39]

Power consumption. Usually, varying between different engines and valve train configurations, the valve train contributes up to 25 percent of the total internal friction. This percentage reduces with engine speed increase. For example, in the study of Valvetrain Friction [40], the members of Automobili Lamborghini, Calabretta and Cacciatore indicates that based on motored strip measurements, valve train contributes 35 percent of total engine components friction at 1000 rpm which is close to the engine speed range of crawling in slow traffic and cursing on the highway. [38]

This percentage can be very significant especially if the valve spring needs to fight harder to eliminate valve floating in high-performance engines. Youd identifies better valve spring dynamic performance with higher internal stresses. [41] Valve floating is mainly caused by resonances in the valve springs. To solve this, up to two additional springs can be sleeved up inside of one other. A Ribbon Damper is also an alternative. However, according to Youd's research, a damper can generate heat and will lead to much higher power consumption. [41]

Limited valve timing, lift and duration. The conventional valve train, either driven by the pushrod or the belt, is required to have a valve actuator known as the camshaft. Figure 6 shows the structure of the camshaft. On the cam shaft, for each valve, there is a cam lobe designed following the specification of the valve opening duration, lift and timing. In other words, the valve motion is pre-set and controlled by the shape, height and angle of the cam lobe. However, in order to accommodate different working

conditions and achieve the optimum efficiency, the valve timing, lift and duration need to have a considerable amount of variation range. [37]

To relatively widen the optimum efficiency range, auto manufacturers and researchers sought various routes for modifying the very basic conventional valvetrain. Fluid-actuated valve systems were quite popular in late 1990s and early 2000s. Renault and Aprilia both created pneumatic valve actuator system to increase valve opening speed and closing force. Renault later also created an electric hydraulic valve actuation system that allows for more advanced valve timing. [42]

However, rarely is any fluid valve actuation system made to the market. More popularly, manufacturers prefer a Desmodromic valve actuating system. They are indeed more reliable, however introduce even more mechanical parts.

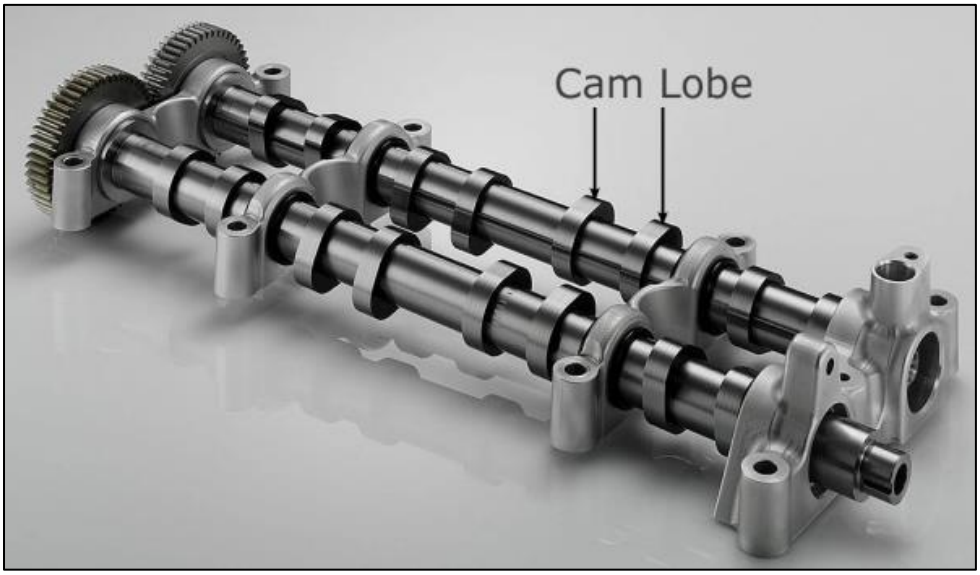

Figure 6: Camshaft Structure [22]

Hence, a novel valvetrain, an electronic rotary valve, is created to eliminate the potential of the valve floating and the valve-train friction by changing the motion type of

the valve and reducing the amount of components driven by the crank shaft. Ultimately, cooperating with wider range of variation, the improvement of the engine efficiency can be achieved throughout the entire power band. The advantages of a rotary valve over a conventional poppet valve are reported in research [19-21] and can be summarized as (1) elimination of reciprocating valve motion can result in reducing frictional power losses of the engine. (2) optimized combustion chambers can be designed using a rotary valve that will provide a high discharge coefficient maximizing the airflow in the combustion chamber. (3) A rotary valve can have a larger cross-section area than an equivalent-sized poppet valve. (4) increased engine power and reduction in fuel consumption can be achieved by eliminating pre-ignition conditions seen in conventional poppet valves. and (5) fewer moving parts in rotary valve design can benefit in reduced costs of manufacturing and maintenance.

The new valve is fitted into the original spaces for the conventional valve. Driven by the overhead electric motor, the valve spins in place to open and close by staggering the vents in the side. Figure 7 shows the novel rotary valve assembly configuration.

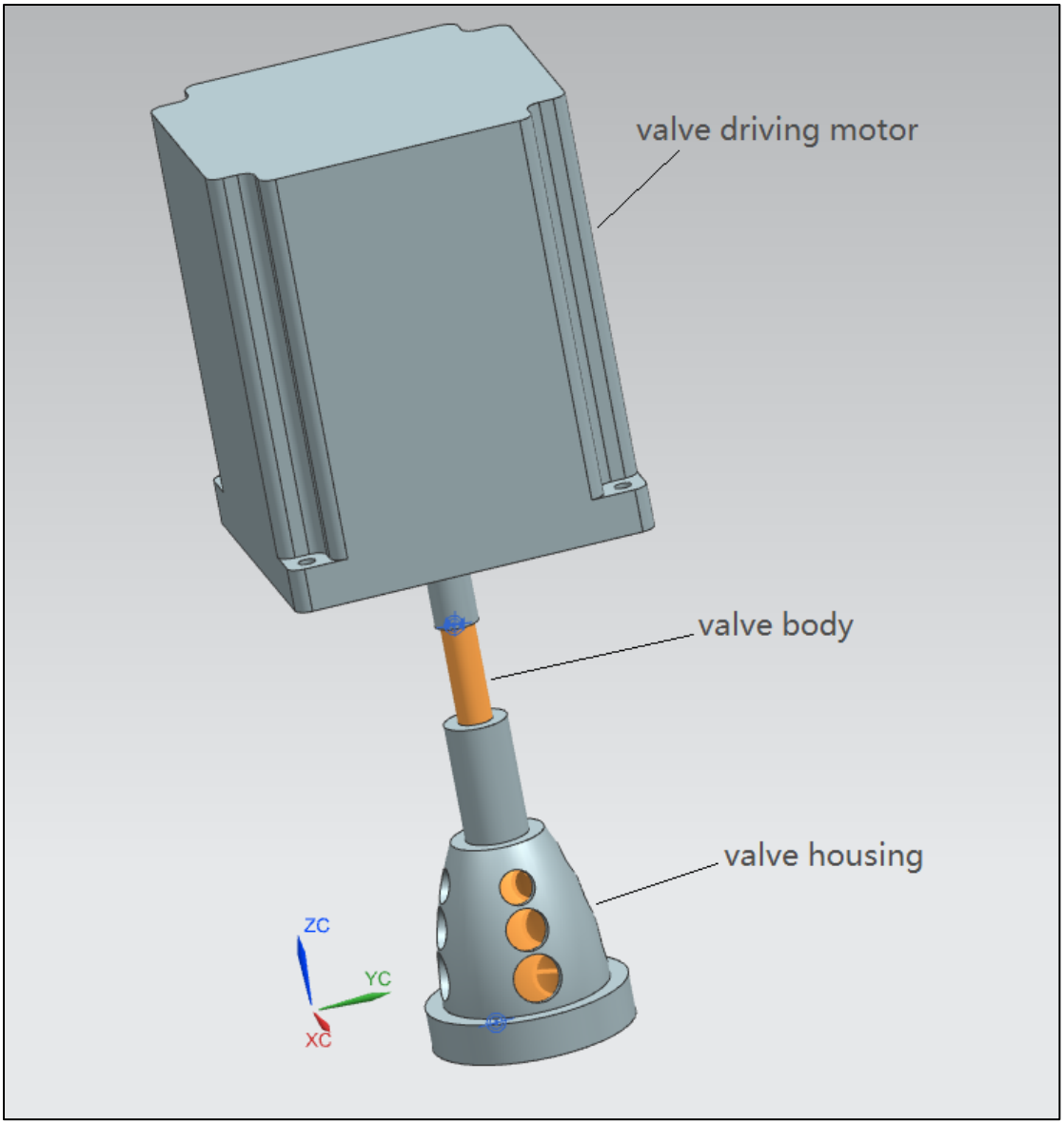

Figure 7: Rotary Valve Assembly Configuration

3.2 FEASIBILITY ANALYSIS

3.2.1 Valve Opening Timing

According to the timing diagram that is shown in figure 8, timing can be addressed down to the crank shaft angles where the valves open or close.

On the selected benchmark engine, the intake valve opens at exact TDC then closes at 207° after BDC. And the exhaust valve opens at 201° before BDC then closes at exact TDC.

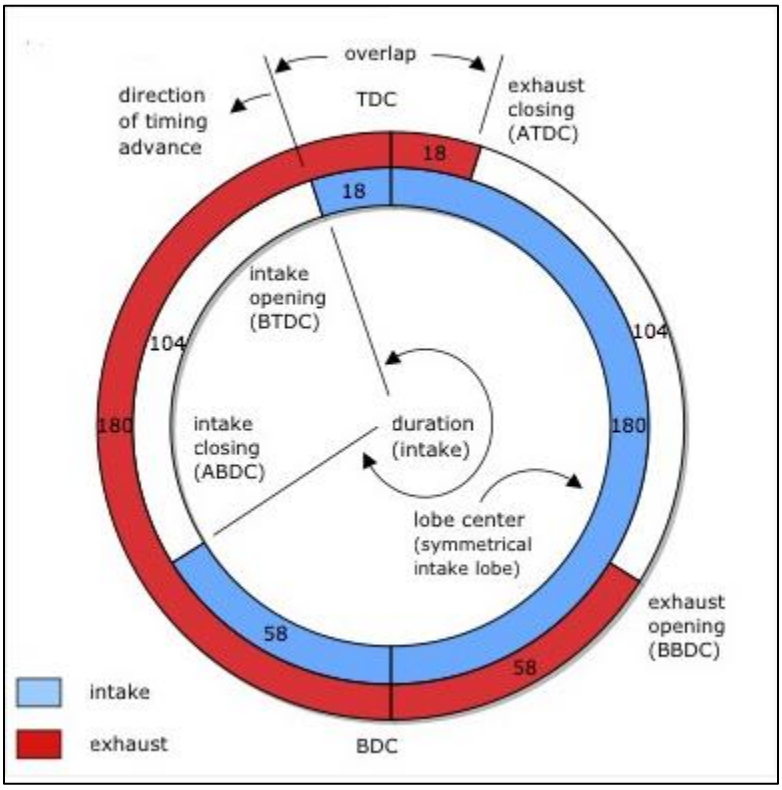

Figure 8: Engine Timing Diagram [43]

3.2.2 Camshaft Related Parameter

Lift and duration are the primary parameters of the camshaft, which determine how high and how long the valve lifts during the operation of the engine. Figure 9 shows the diagram of the camshaft cross-section.

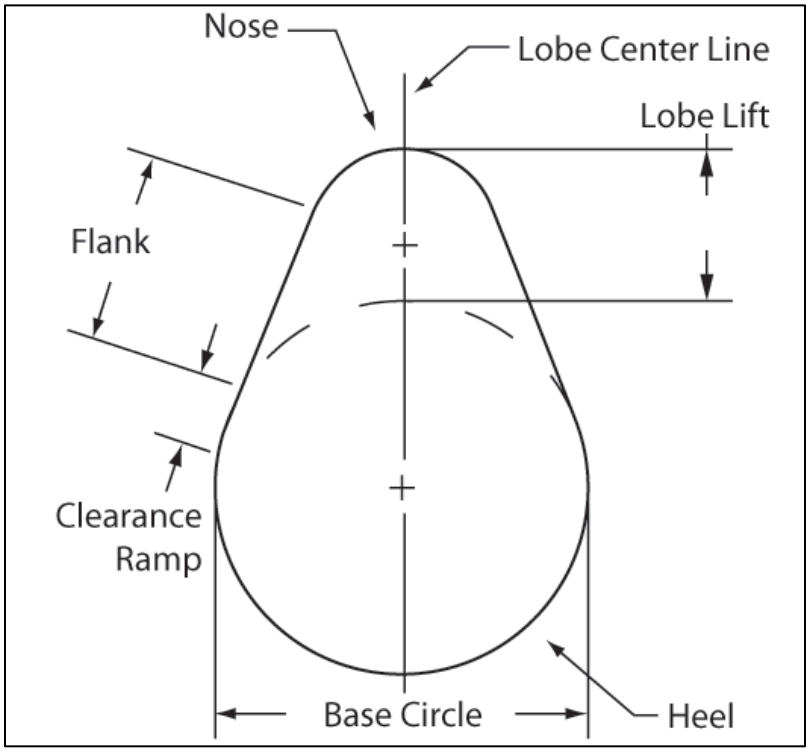

Figure 9: Cam-lobe Diagram [44]

3.2.3 Lift

Valve lift refers to the maximum distance covered by the valve during the opening process. This measurement is determined by calculating the disparity between the maximum height of the cam-lobe and the size of the cam-lobe base circle. Occasionally, the valve lift can be magnified by the rocker arm, which amplifies the height of the camshaft lobe. In the context of this study, the initial valve lift is equivalent to the maximum lift of the cam-lobe multiplied by the rocker arm's augmentation

ratio.

$$l = l_l r_a \tag{1}$$

In which, l stands for the valve lift while l_l and r_a represent the lobe lift and the rocker arm ratio.

On the benchmark engine, the camshaft lobe's maximum sizes are 1.341 in. (intake) and 1.27 in. (exhaust) and the lifts are thus 0.241 in. (intake) and 0.227 in. (exhaust). The measured magnifications for both rock arms are 1.335. The intake and the exhaust valve lifts are 0.322 in. (intake) and 0.303 in. (exhaust), respectively. [38]

3.2.4 Valve Opening Area

The valve opening area is determined as the curtain area by multiplying the valve lift and the circumference of the valve head, within the critical condition. According to measurements of the original poppet valves, the valve head diameters for the intake and exhaust are 1.3 inches and 1.1 inches, respectively. Consequently, the valve opening areas for the intake and exhaust valves are 1.314 square inches and 1.047 square inches, respectively. When the curtain area is equal to the valve port area, the valve opening area is considered as the port area.

3.2.5 Duration

The duration of valve opening is determined by the period the valve remains open, and it is measured in crankshaft angle. This duration is assessed from when the valve is lifted 0.050 inches to when it is 0.050 inches away from complete closure. In this particular scenario, the intake valve duration is 207°, while the exhaust valve duration is 201°.

To ensure a smooth rotation of the camshaft lobe and proper valve operation, a transition from the base circle to the maximum lift height is essential. Consequently, the valve's motion is gradual, especially at the beginning and end of its movement. This study concentrates on the performance of the intake valve, so only the intake side is examined. Figure 10 shows the measured valve lift curve, indicating a maximum valve lift of 0.322 inches for the intake valve, aligning with the calculated results.

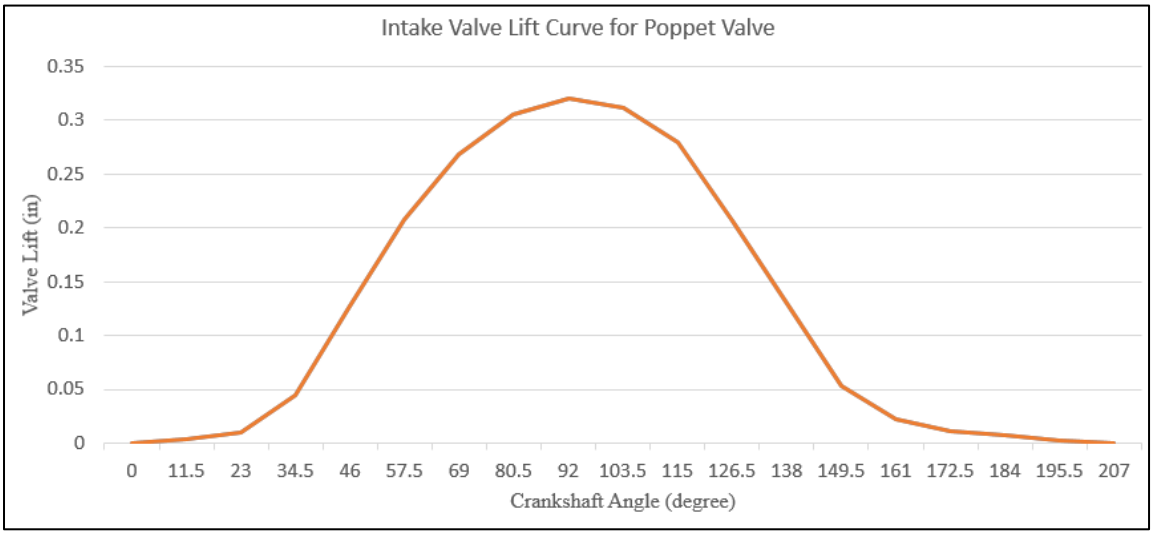

Figure 10: Poppet Valve Lift Height Curve

3.3 Requirements of the new valve design

To show that a new design is significant, at least the original valve performance has to be met. Under this circumstance, the gas exchange capacity is the key factor of the performance. In another word, matching the design of the gas exchange capacity becomes the goal of the research.

The rotary valve offers a notable advantage by delivering a sharp and linear valve motion curve. While the physical port of the valve may not reach its original area, the primary goal of valve improvement extends beyond the emphasis on the valve opening

area. The true objective is to enhance the quantity of air aspirated into the cylinder, a factor intricately linked to volumetric efficiency.

In contrast to the traditional valve motion, where attention is typically confined to the effective valve lifting range, a more comprehensive approach considers the entire span from the initiation to the culmination of the valve motion. This broader perspective encompasses the entire mass of air exchanged by the valve. Unlike the conventional valve, which experiences a wasteful duration during the ineffective valve lifting range due to its smooth transition, the rotary valve is specifically designed to facilitate a sharp and precise valve opening and closing. Consequently, the smooth transition characteristic is eliminated in the rotary valve design.

3.4 Design details

3.4.1 Timing and duration

Ultimately, the new design has the ability to achieve unlimited timing and duration variation. However, in this research, since the goal is set to match the design of the benchmark engine, the timing and duration settings remain as the original engine measurement.

3.4.2 Lift and valve opening area

The rotary valve operates on engine speed-related rotational stagger motion, so the term lift is no longer applicable. However, the shape of the opening port does contribute to performance variation. Thus, the lift can be replaced as opening and closing duration which describes the speed of valve operation.

As discussed, one feature that the rotary valve provides is the sharp valve motion curve which can be translated into fast valve motion. The feature provides the engine with a wider range of effective gas exchange duration.

3.4.3 Valve shape

In order to accommodate the original Suzuki engine cylinder head, the intake valves must fit into the space of 1.386×1.386×2.2 inches. The optimum shape of the valve application is hemisphere which evenly distributes the force between the valve body and its housing under the combustion cycle. Limited by the size of the space, however, the valves are finalized into a cone shape with a curved surface to prevent self-seizing under heavy load.

In this typical design, the opening ports are made into true circles with three different radii of 0.119,0.148, and 0.165 inches to accommodate the shape of the valve.

3.4.4 Driving mechanism

Instead of using the traditional timing components, the rotary valve is driven by the overhead stepper motor. With a timing trigger wheel mounted on the crankshaft and a correlated crankshaft position sensor, the engine control unit is able to sense the exact angle of the crankshaft and trigger the steeper motor to drive the valve accordingly to time the motion.

3.5 Method

In order to identify the improvement of the performance of the new valve design over the conventional valve, several parameters can be applied to the measurement. In this research, modifications are made to both the shape of the valve body and its port, resulting in changes to the motion type of the valve. One major change that resulted is the volumetric efficiency. On the internal combustion engine, higher volumetric efficiency allows the air to flow easier. In other words, the cylinder is able to aspirate more air within the same crank rotation angle.

Since the major change in the structure is the valve shape and motion type, the most direct result is the change of the valve opening area curve. Thus, in this research, instead of focusing on the overall volumetric efficiency table, the individual efficiency curve for one cycle of the valve motion is presented. Comparing this curve between the new design and the conventional design, it is easy to identify the difference in the performance.

3.6 Program design

Volumetric efficiency is the ratio of the actual aspirated air volume and the physical cylinder volume. -

$$\mu = \frac{V_a}{V_d} \tag{2}$$

In which, V_a stands for the actual volume of intake air while V_d represents the theoretical volume of the cylinder. [45]

The benchmark engine is an indirect-fuel-injection engine. However, since the amount of fuel is small enough compared with the amount of air, the fuel mass can be neglected for volumetric efficiency calculation. [46]

In equation 3, the actual intake air volume can be presented as the function of air mass and air density.

$$V_a = \frac{m_a}{\rho_a} \tag{3}$$

On the engine dynamometer, air mass is usually replaced by intake air mass flow rate. [26]

$$\dot{m}_a = \frac{m_a N_e}{n_r} \tag{4}$$

Where, N_e stands for engine speed and n_r is number of crankshaft rotations for a complete engine cycle.

Intake air pressure and temperature are usually measured in the intake manifold so the intake air density can be calculated as the following equation.

$$\rho_a = \frac{P_a}{R_a T_a} \tag{5}$$

Where, ρ_a is intake air density, P_a is intake air pressure, T_a is intake air temperature and R_a is gas constant for dry air.

Replacing 4 and 5 in 3 gives the volumetric efficiency equal with the following equation.

$$\mu = \frac{\dot{m}_a n_r R_a T_a}{P_a V_d N_e} \tag{6}$$

In this research, the major change of the improved design compared to the benchmark engine is the valve shape and its motion type. As a result, the valve flow and

discharge coefficients are the most essential effects of the volumetric efficiency. Thus, only the intake performance will be evaluated. [47]

The mass flow rate through a valve is usually described by the equation of compressible flow going through a flow restriction.

$$\dot{m} = \rho_o c_o A_E \left(\frac{P_T}{P_O}\right)^{\frac{1}{k}} \left\{ \frac{2}{k-1} \left[1 - \left(\frac{P_T}{P_O}\right)^{\frac{k-1}{k}} \right] \right\}^{\frac{1}{2}} \quad (7)$$

In which, P_o and ρ_o stand for upstream stagnation pressure and density, respectively. $c_o = \sqrt{kRT_o}$ stands for sound speed with T_o stands for temperature. A_E is effective area of valve assembly. And P_T represents downstream static pressure. [48]

For flowing into the cylinder, P_o and P_T are the intake system pressure and the cylinder pressure respectively.

Introduce 7 into equation 6 and keep the valve opening area A_E as the variable, the relationship between the valve opening area and the instant volumetric efficiency can be described.

3.6.1 Valve opening area

Figure 11 shows the design of the rotary valve. In the new design, linear motion no longer exists hence the curtain shape opening port. The valve has three different sized round ports in every 90 degrees. Driven by an electric motor, for every 45 degrees of rotation, the valve completes its opening and closing. In order to perform a proper curve of the opening area change, the three ports in a row opens and closes at the exact same time.

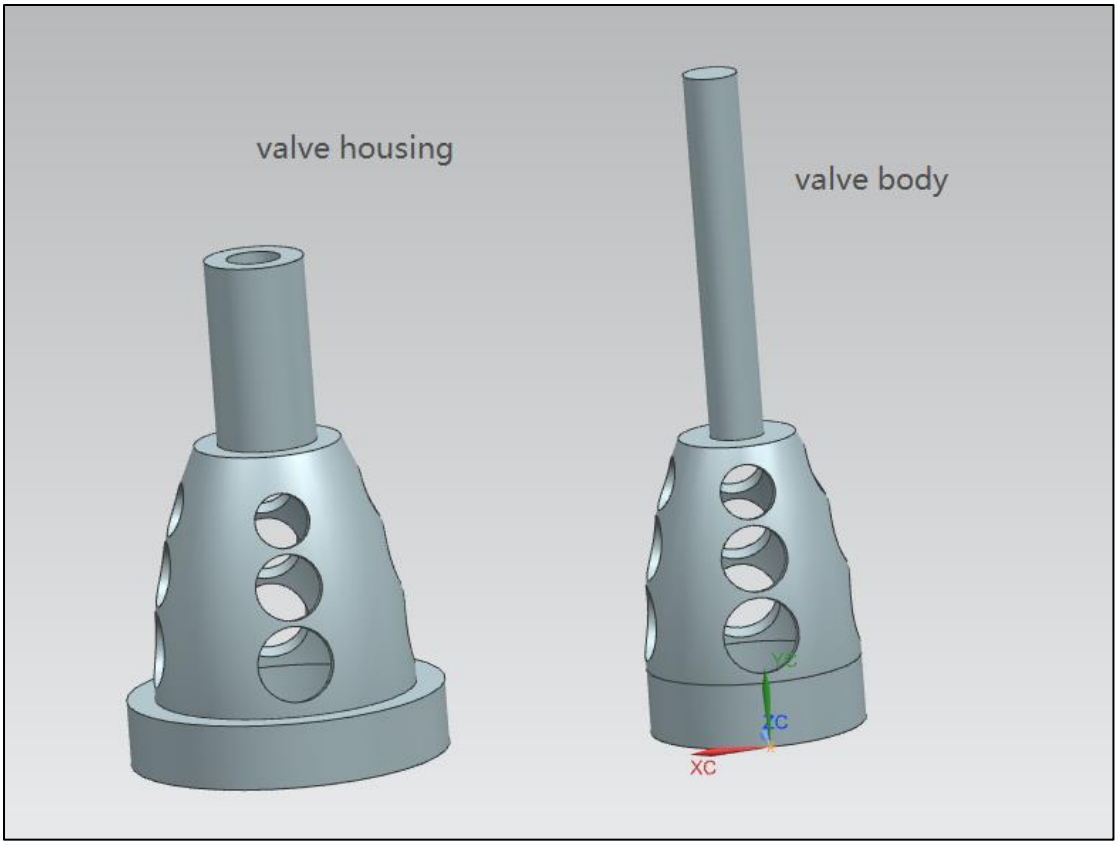

Figure 11: Rotary Valve

In order to calculate the effective valve opening area and present the motion curve, the system is simplified into the area problem of a line sweeping across a circle as shown in Figure 12. In this case, the valve opening area is described as the sum of the truncated circle areas.

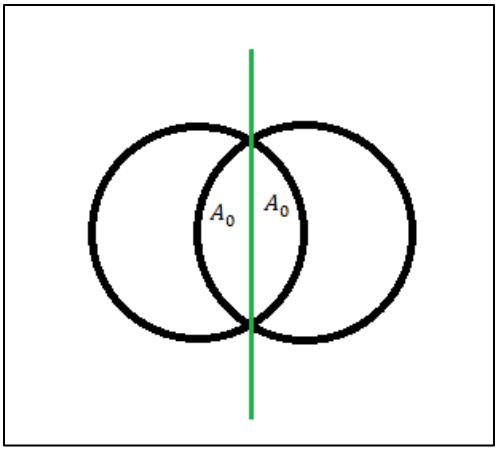

Figure 12: Simplified Valve Opening Problem

$$A_0 = \arccos\left\{\frac{r-d_o}{r}r^2 - \left(\sqrt{r^2-(r-d_o)^2}(r-d_o)\right)\right\} \tag{8}$$

Where, r stands for valve port radius.

Since the valve housing and core both have the same size port, the valve opening area is twice as the truncated circle area.

$$A = 2(A_{01} + A_{02} + A_{03}) \tag{9}$$

d_o, in equation 8, represents the linear distance traveled by the valve ports. A_{01}, A_{02}, A_{03} represent the A_0 of the 3 port holes respectively. In this research, since the variable valve algorism is not introduced, the valve motion and the crankshaft rotation angle are still considered as related.

$$d_0 = \frac{\theta v_v \pi R}{360 N_e} \tag{10}$$

In which, v_v and R represent the valve rotation speed and radius of the valve port orbital.

To complete the comparison between the new design and the old design, the same curve of the conventional valve is needed too.

Based on the valve shape and its motion type, the poppet valve has a circular cap that moves up and down to modulate the valve opening and closing. During the valve opening, the edge of the circular valve draws a cylindrical curtain shape and the area of the curtain is the instantaneous valve area. [45]

$$A = \pi d_v l \tag{11}$$

Where, d_v and l represent valve diameter and valve lift. And both parameters are obtained from the actual measurement. Apply the data points of valve lift to the method of polynomial approximation, the valve lift to the function of crankshaft angle can be obtained. Table 1 and 2 shows the coefficients of the 14-degree and 15-degree polynomial approximation. Figure 13 and figure 14 shows poppet valve opening area predictions.

Table 1: 14-Degree Polynomial Approximation Coefficients of Poppet Valve Lift Curve

1.34057576152852e-29	-1.97553920205812e-26	1.46162855199868e-23
-7.37941269758326e-21	2.74879288704423e-18	-7.49437859202936e-16
1.45815618211744e-13	-1.97909977340450e-11	1.82797615744295e-09
-1.10629478732787e-07	4.10232387967087e-06	-8.27649925543051e-05
0.000792266345094215	-0.00231720481869556	0.000147178187343951

Table 2: 15-Degree Polynomial Approximation Coefficients of Poppet Valve Lift Curve

8.72448957224518e-30	-1.35313642804956e-26	9.45434850116815e-24
-3.93036276539530e-21	1.08112500700193e-18	-2.06876504858949e-16
2.81579223001290e-14	-2.73591172698436e-12	1.87301430848427e-10
-8.74677136652550e-09	2.62475776957364e-07	-4.57848868734980e-06
4.04649013154706e-05	-0.000135047970803517	0.000360469542360491
4.54797548741340e-05		

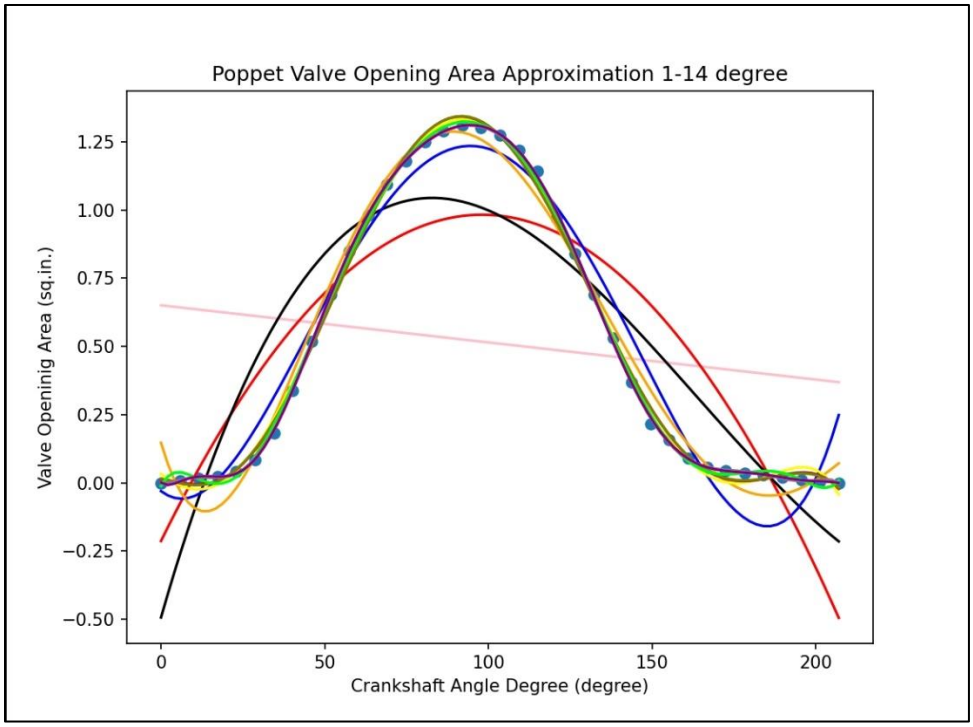

Figure 13: Poppet Valve Opening Area Approximation 1-14 Degree

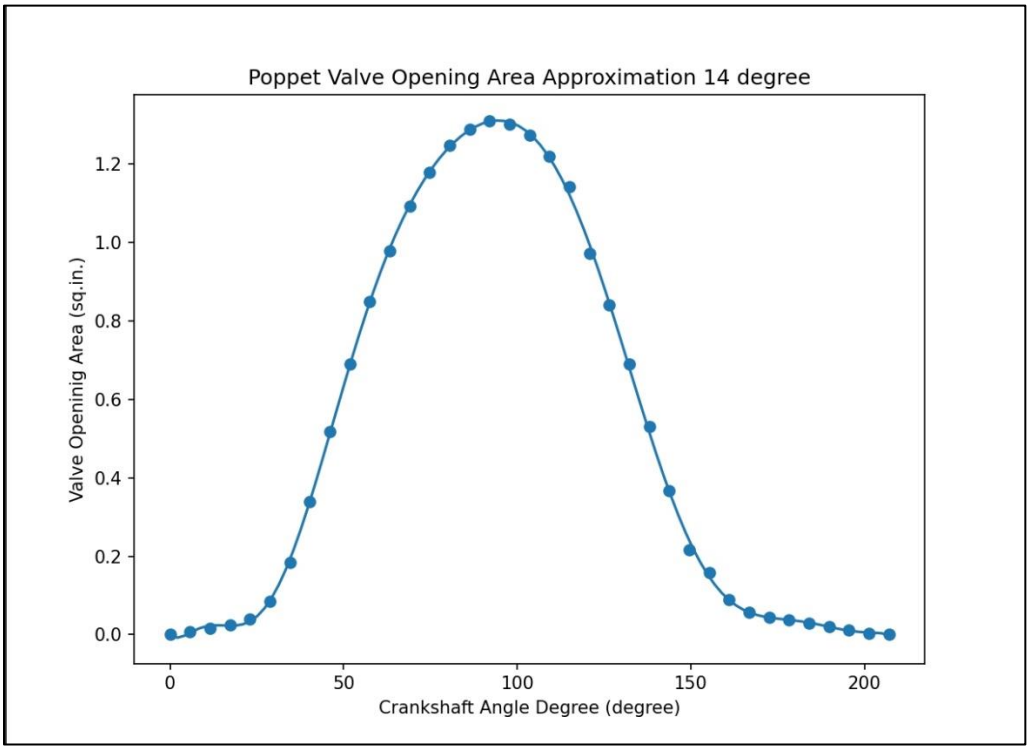

Figure 14: Poppet Valve Opening Area Approximation 14 Degree

The approximation is then validated with cross-validation. Since the dataset is linear, randomization to the dataset was expressed so the k fold split process does not break the data consistency.

In this study, $k = 5$ was selected to split the data into 20/80 ratio. Prediction runs on the 80% fitting data to generate the fitted equation. 20% test data is saved to validate the prediction outcome. Figure 15 and Figure 16 show one example of 80% data prediction for 1-14 degree polynomial approximation and 14 degree polynomial approximation.

The cross-validation runs 5 times with each group testing data passing into the outcome for validation. Table 3 and Table 4 show the result.

Table 3: 13-Degree Polynomial Approximation Cross-Validation Result

No. of run	Mean squared error (MSE)	Average MSE	MSE standard deviation	MSE standard error	95% confidence interval
1	0. 4693	0. 4950	0. 1788	0.0799	0.4950±0.1567
2	0. 6278				
3	0. 1857				
4	0. 4835				
5	0. 7087				

Table 4: 13-Degree Polynomial Approximation Cross-Validation Result

No. of run	Mean squared error (MSE)	Average MSE	MSE standard deviation	MSE standard error	95% confidence interval
1	0. 2816	0. 1762	0. 0738	0.0330	0. 1762±0.0647
2	0. 1082				
3	0. 0952				
4	0. 1537				
5	0. 2428				

The k-fold cross validation for the 14-degree polynomial resulted in a mean MSE of 0.1762 +/- 0.0647where the 95% confidence interval was calculated using the standard error of the mean. 14-degree approximation result is selected for future evaluation.

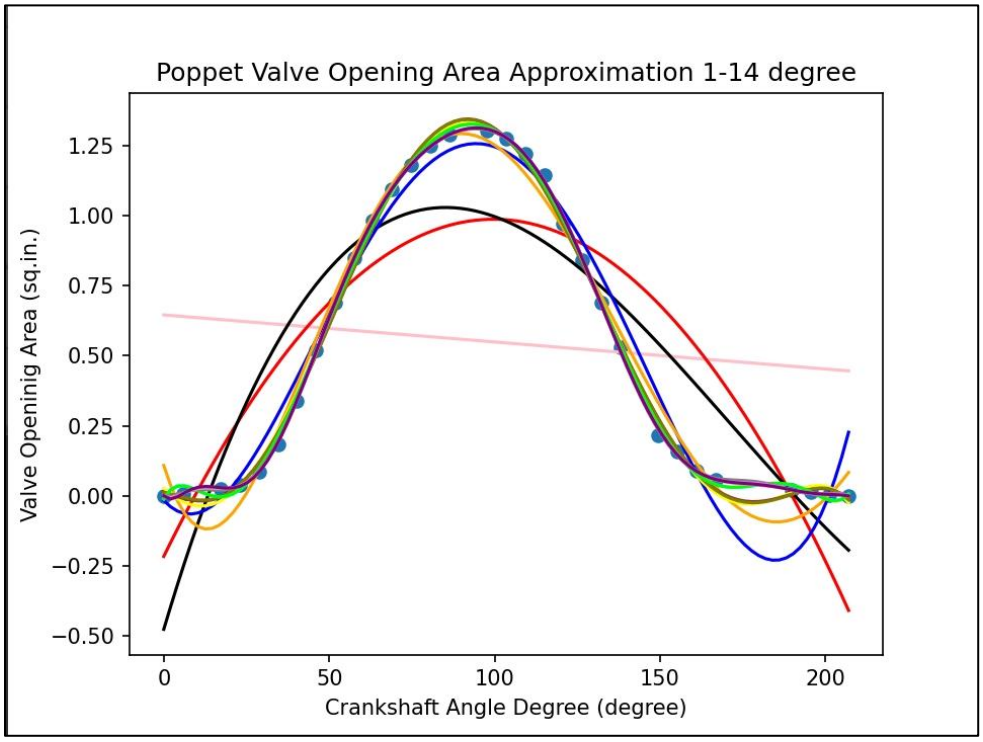

Figure 15: Poppet Valve Opening Area 1-14 Degree Cross-Validation

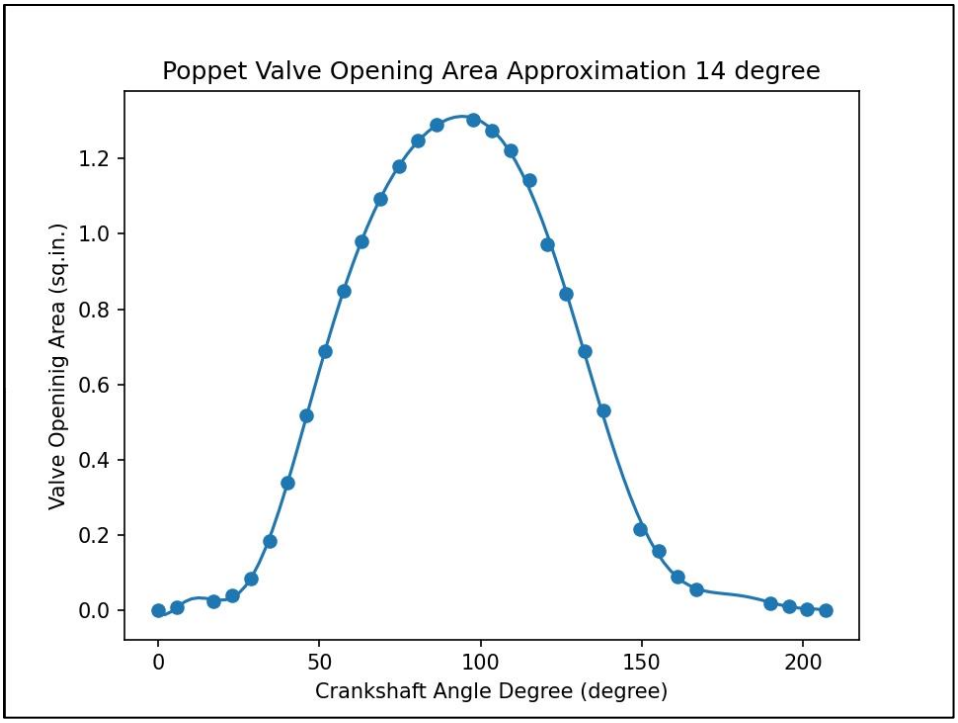

Figure 16:Poppet Valve Opening Area 14 Degree Cross-Validation

3.6.2 Saturation point

At somewhere in the mid-range of the valve lift, the saturation point of the port is achieved. After this point, the valve curtain area goes beyond the size of the valve seat area and the flow restriction moves from the valve curtain to the actual port itself.

At this point, the valve opening area becomes the valve seat area.

$$A = \pi r^2 \tag{12}$$

3.6.3 Discharge and flow coefficient

The effective valve opening area defines the mass flow rate through the valve, which is the product of the reference valve area and the valve discharge or flow coefficient.

For the conventional valve structure, the discharge coefficient will be applied if the reference valve area is set to be the curtain area. Otherwise, the flow coefficient becomes applicable if the reference valve area is the seat area. In this research, the flow coefficient was adopted through a polynomial approximation of GT-Power simulation. [45]

$$A_E = CA_r \tag{13}$$

$$C_f = -0.001 + 3.5477\frac{l}{d} - 6.566\left(\frac{l}{d}\right)^2 \tag{14}$$

While on the new rotary valve design, since the valve opening area is determined only by the opening condition, equation (9), critical condition is no longer necessary to be considered.

The conventional numerical simulated equations are no longer applicable. However, since the structure of the valve opening ports is shaped into circles, the equations of the nozzle and orifice flow coefficient became suitable for this application.

The nozzle or orifice is used to reduce pressure. In this case, however, becomes the restriction of the airflow.

$$C_d = C_\infty + \frac{b}{{R_e}^n} \tag{15}$$

Referencing the physical design of the rotary valve, the device type can be identified as “orifice, corner taps”. The discharge coefficient is defined as the above equation, where C_∞ stands for discharge coefficient at infinite Reynolds number, β stands for area ratio, R_e stands for the Reynolds number, b and n are the coefficients found in the chart from reference [49]

$$C_\infty = 0.5959 + 0.0312\beta^{2.1} - 0.184\beta^6 \tag{16}$$

$$b = 91.70\beta^{2.5}, n = 0.75 \quad (17)$$

3.7 Results and Discussion

Since the conventional poppet valve operates related to the camshaft rotation angle. The valve opening area curve remains invariable under any engine speed. Figure 17 shows the intake valve opening area curve of the poppet valve.

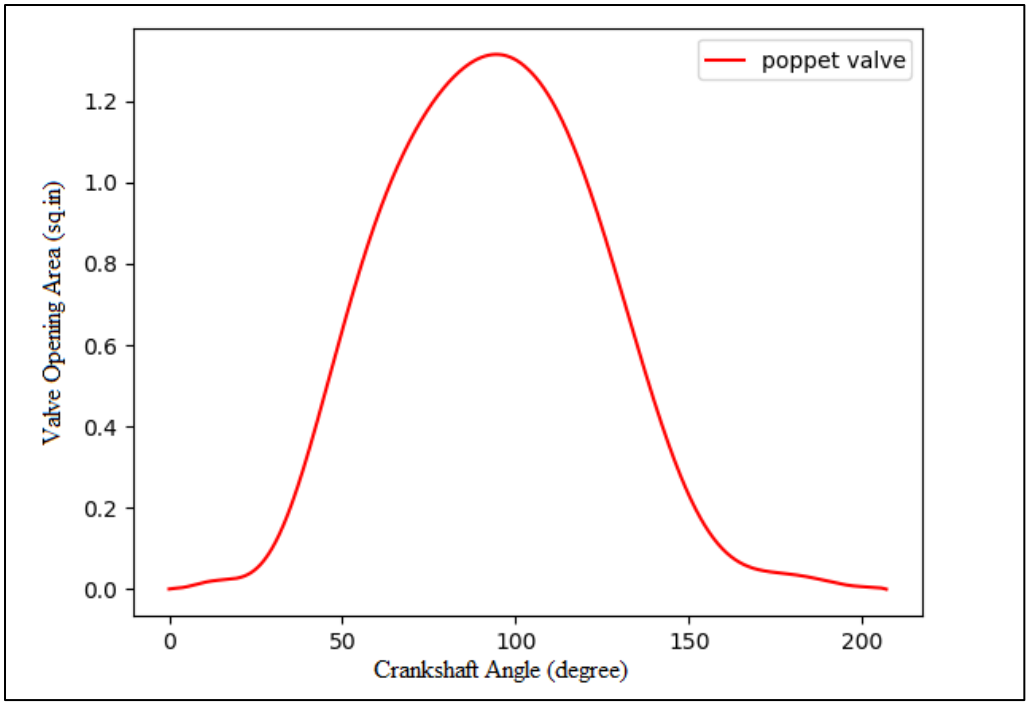

Figure 17: Intake Valve Opening Area Curve for Poppet Valve

However, the rotary valve is designed to be driven by an electric motor under the motor's constant speed. Once the valve completes its opening operation, the motor stops and keeps the valve remaining open then drives the valve close per command of the engine control unit. Limited by size, it is expected that the new valve design provides a smaller opening area. Nevertheless, the valve opening duration is increased. Figure 18 shows the valve opening area curve of the rotary valve in three dimensions. According to

the calculation, the maximum opening area for the rotary valve and the poppet valve are 0.795 sq.in and 1.315 sq.in.

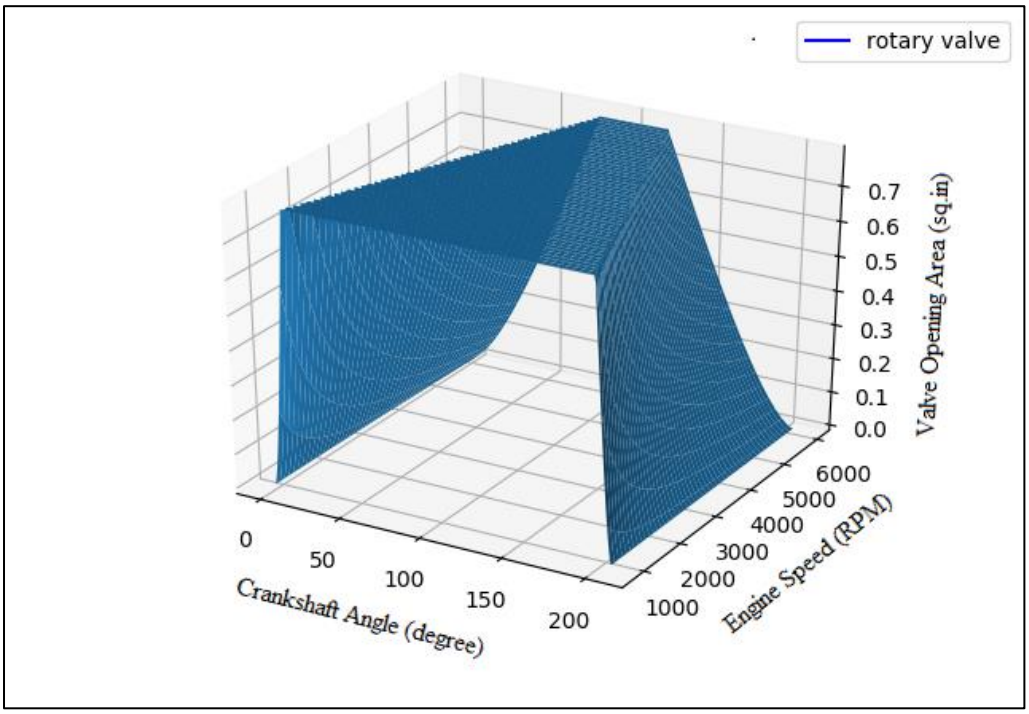

Figure 18: Intake Valve Opening Area Curve for Rotary Valve

Since the valve operation speed remains constant, with the engine speed increasing, it is obvious that the maximum valve opening area duration reduces. Eventually, the electric motor is not able to catch up with the engine speed and the valve is not able to reach its maximum opening area.

Instead of focusing on the overall valve assembly efficiency, this research calculates the instantaneous efficiency during the valve opening process.

Limited by the motion type and cam lobe profile, the conventional poppet valve has to open and close gradually before reaching maximum efficiency. In another word, during the beginning and the end of the motion, the valve has to run under a very

inefficient condition and can barely aspirate any air. Furthermore, due to the fixed timing system, the poppet valve can only maintain its higher efficiency for a relatively narrow range. However, on the rotary valve design, depending on how quick the valve motor operates, the rotary valve is able to complete its maximum area opening within a smaller crankshaft angle interval. Figure 19 shows the both instant efficiency curve of the poppet valve and the rotary valve at the engine speed of 2900 RPM.

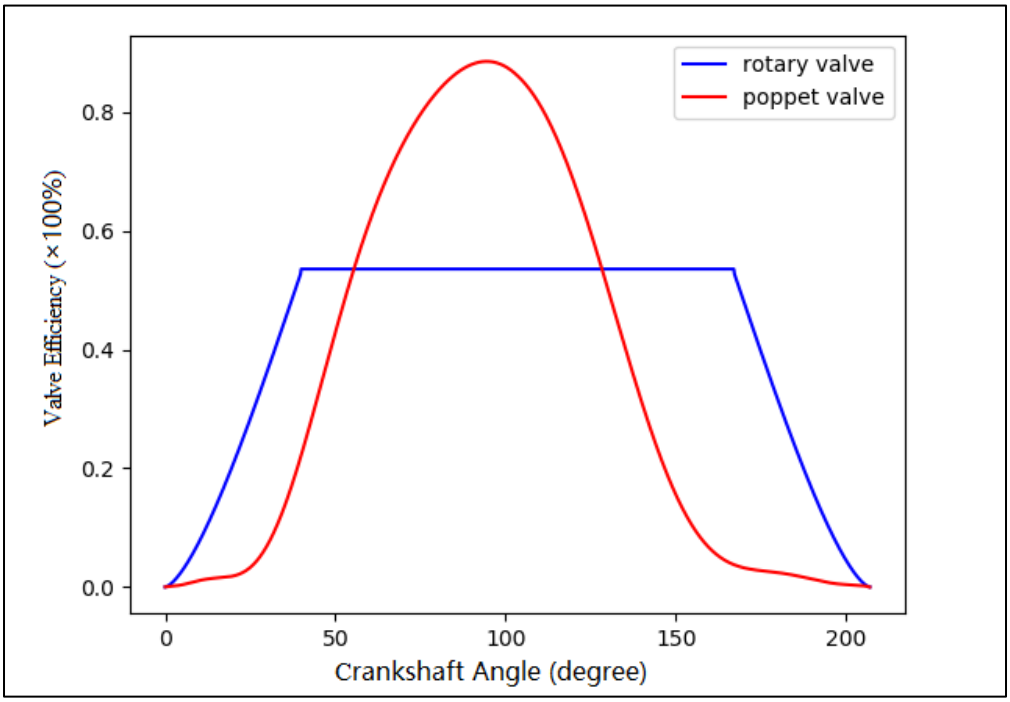

Figure 19: Instant Efficiency Curve under 2900 RPM

However, due to the performance limitation of the valve driving motor, the valve is not able to reach its maximum efficiency. With the engine speed increasing, the time interval of the intake stroke reduces. Since the valve-driving motor operates under its specified speed, the engine control unit has to command the valve to start to close before the maximum opening area is completed. According to the calculation, the rotary valve

design and the conventional poppet valve design achieve very similar performance at 4400 RPM. Then, after 4500 RPM, the poppet valve performance exceeds. Figure 20 shows the efficiency curve at 4400 RPM. The aspirated air volume ratio between the popped valve and the rotary valve are 0.850 and 0.996 at 2900 RPM and 4400 RPM, respectively.

As mentioned earlier, the maximum opening area for the rotary valve is calculated to be 0.795 sq.in which is smaller than the poppet valve's area of 1.315 sq.in. However, under 2900 RPM engine speed, the rotary valve is able to remain fully opened with a constant efficiency of about 54% from 40 to 160 degrees of the crankshaft angle. While the poppet valve can achieve 88% efficiency at 90 degrees of the crankshaft angle, the efficiency significantly drops on either side of the maxima.

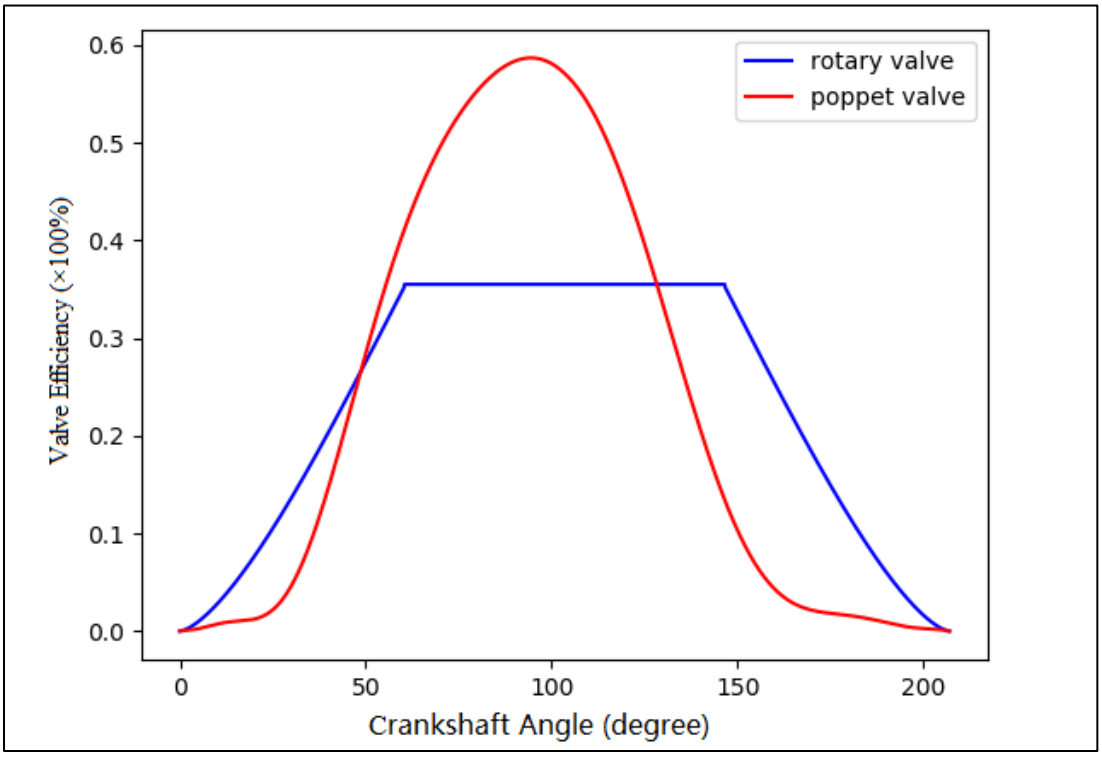

Figure 20: Instant Efficiency Curve Under 4400 RPM

3.8 Conclusion

Based on the modeling, simulation and design of experiments, the study distinguishes the advantages and the limitations of the new proposed rotary valve design. This design enables maximum opening of the valve for a longer duration and hence has the potential to enhance efficiency of the engine. However, in this research, limited by space, the new design that is constructed based on the existing engine head can not compete on the maximum opening area with the conventional design.

Modifications that make horsepower and torque in the lower rpm range between 1500 and 3000 rpm are way more useful than a high-revving race motor and most modern civilian use vehicles run at 2000-3000 rpm when cruising at a speed of 70 mph. The literature review also shows that engines obtain their optimum efficiency at lower engine speeds. In this research, it is found that the proposed rotary valve design provides a constant efficiency of 54% for a much larger crankshaft angle duration compared to the conventional poppet valve design under 2900 RPM engine speed.

Based on the calculations, the rotary valve design achieves better performance below 4500 RPM, and it will contribute towards the reduction of the engine internal friction by eliminating the entire valve driving mechanism. Compared to other rotary valve designs, the proposed design in this study offers a shape that is naturally mechanically sealed. The intake and the exhaust side valves are independent. The electronic control concept offers a fast-opening speed and longer duration. The concept is also significant for future research on wide-range variable valve timing systems and high compression interference-free engine design.

CHAPTER 4 DESIGN, MODELING AND SIMULATION OF AN IMPROVED ROTARY VALVE INTERNAL COMBUSTION ENGINE

4.1 Introduction and Literature review

The research and analysis demonstrated in previous section show brief evidence of a significant feasibility of the rotary valve and highlights the discussed design can benefit the most daily used engine speed range. Although it may not be the most efficient and optimized construction, the idea frees up more possibilities of the rotary valve.

Despite the increasing popularity of electric vehicles, numerous major auto manufacturers have affirmed their commitment to persist to ongoing research and production of internal combustion engines (ICE).

Volkswagen in 2021 stated that they would stop internal combustion engine development and production by 2026 and move to EV only by 2035. However, at the beginning of 2024 they reaffirmed not to abandon their ICE vehicle products and reported that more plug-in hybrid vehicles would be added to the line. [50, 51]

Mercedes in 2021 revealed that they would speed up their EV-only plan and issue an EV-only platform by 2025 then be fully ready for EV-only by 2030. However, the plan quickly became ICE and EV parallel in 2023. Later in 2024, Mercedes indicated there will be a brand-new ICE vehicle line in 2027 and ICE vehicle sales will continue till at least 2030. [52-54]

Ford postponed its $12 billion EV investment in 2023 and further cut back F-150 Lightening electric truck production in 2024. [55, 56]

Statistics show over 50000 research publications discussing internal combustion engines since 2018 and over 14000 topics are related to various types of rotary valve engines.

Mason and Lawes proposed a vertical mono-rotary valve design in 2022. The cylindrical shaped valve was located on top of the piston spinning vertically in place with cutout from the side to the bottom connecting the combustion chamber to either the intake port or the exhaust port. The valve operated under a fixed timing driven by a series of gears, bearings and shafts in between the valve and the crankshaft. The research proposed two valve sizes with one being able to match the conventional poppet valve performance while the oversized one provided better gas exchange. However, with their set valve diameter, in order to achieve better performance, the valve had to be made much taller which enlarges the combustion chamber volume and reduces the compression ratio.[57]

Deng's team presented a single rotary valve engine design in 2020. Like Mason's rotary valve, Deng's valve was also cylindrical shaped but with a cutout in the side only connecting the cylinder to either the intake port or the exhaust port. The valve was positioned horizontally and spin in place around its center axis. Differing from the vertical rotary valve with the inner space being a part of the combustion chamber, the horizontal rotary valve did not generate extra combustion volume. Thus, the combustion chamber was designed into a more optimized shape and obtain a higher compression ratio. However, since the single valve functions as intake and exhaust valves, variable timing became impossible.[58]

In the same year of 2020, Deng's team also developed a double rotary valve engine design. With the same valve body construction, the double rotary valve engine fitted a larger and a smaller valve in the cylinder head for intake and exhaust respectively. According to the research, the double rotary valve design reduced the amount of valvetrain parts to 50 compared to the conventional valvetrain's 240 if applied to a four-cylinder engine and on their specific design, the compression ratio could reach up to 18:1.[15]

In Brown's study in 2014, with the novel floating valve seal, a two-port single rotary valve was introduced. The valve was cylindrical shaped, positioned horizontally with two through round ports in the side for intake and exhaust respectively. The valve was designed to spin in place aligning the ports to open and close the intake and the exhaust ports. Although the valve was designed to be used in pneumatic applications, it was possible to be a foundation to further develop internal combustion engines.[29]

In 2011, Behrens introduced a unique valvetrain that contains both a rotary valve and a poppet valve named mono-valve. Instead of using multiple smaller poppet valves for intake and exhaust, mono-valve had only one bigger poppet valve to let the gas flow in and out of the cylinder. The rotary valve part was on top of the poppet valve and functioned as a divider to either open to intake or exhaust port. The engine prototype was able to run under its own power. However, the performance of the prototype was not competitive with a conventional engine of the same size. The research did prove the new design benefits the backflow problem. [59]

Robinson and his team posted a study in 2022 on computational fluid dynamics investigation comparing the performance between conventional poppet valvetrain and

rotary valvetrain. The experimented example was a single rotary valve with two ports for intake and exhaust. The valve was cylindrical and positioned horizontally. The valve ports were through holes in the side of the cylinder. Multiple CFD turbulence models showed higher CFM numbers on rotary valves. The discharge coefficient for the rotary valve was able to reach up to 0.97 when fully opened. The total mass flow during the opening duration for the rotary valve was higher despite it having a smaller opening area. The rotary valve outperformed the poppet valve by 52% in intake and 23% in exhaust.[20]

The review paper published by Roodink in 2016 went through multiple valvetrain concepts available for higher performance usage. It was clearly stated that overhead valve concepts need fewer components to overcome the distance between the camshaft and the crankshaft. The extra flexibility and mass in the components made it unstable for high-speed applications.[42]

Bari presented a review study in 2020 on improving airflow characteristics inside the combustion chamber of diesel engines to improve higher viscous fuel burning performance. It was found that 1.3-2.8% efficiency can be extracted from higher turbulence. And traditional methods of increasing turbulence include using guide vanes, throttled intake manifold, optimized combustion chamber shape and modification of intake manifold tunnel. Researchers also found up to 12% improvement in fuel economy by improving the swirl of the flow.[60]

Nakano coupled CFD and AI in 2023 and delivered a study on combustion chamber shape optimization. The optimized combustion chamber was applied to a new engine under development and the result showed significantly lower emission and lower

fuel consumption. The output range and lineup were both improved while keeping a similar footprint and cost to the existing models.[61]

In 2022, Waghmare performed an engine simulation to predict engine performance using Python. Heat transfer, combustion and frictional losses were evaluated.[62]

Calabretta and Cacciatore from Automobili Lamborghini conducted research in 2010 on valvetrain modeling, analysis and measurement. VALDYN was used to create the dynamic mode of a single valvetrain. It was found that friction losses are dominated by losses at the cam/tappet contact at low engine speed. Tappet/bore interface friction losses were worth considering but less important.[40]

Beloiu published a two-part study in 2010 discussing the modeling and analysis of valvetrains. The research created the valvetrain kinematics and optimized the cam shape. Mathematical modeling was constructed for the valve spring, hydraulic lash adjuster and a few other components. Different modeling approaches of valvetrain dynamics were compared and benefits were highlighted. Later in part two, the study went into modeling and simulation of variable timing systems and variable valve actuation mechanisms. The control theories were also presented.[63]

Kakaee and the team developed a novel volumetric efficiency model in 2017 for spark ignition engines with variable valve timing and lift. In the study, they confirmed that a more accurate estimation model is necessary, particularly for engine designs with variable valve technology. A novel semi-empirical model was proposed for volumetric efficiency, which can be calibrated with very few experimental data. It takes valve timing, engine speed, intake manifold pressure and valve lift as the input data to the

model. The model was validated by six different engines to further prove its generalizability.[64]

4.2 Current work and problems

The significant increase in engine development costs, combined with the focus on optimizing poppet valves, has diverted attention away from innovative engine valve systems. In fact, numerous major automakers have explored alternative avenues, exploring rotary valve technologies and securing patents; however, very few have shared their findings publicly. [65]

At the time of this research, only a few companies have tried commercializing their rotary valve innovation.

4.2.1 The Bishop Rotary Valve

In the early 1990s, Bishop Innovation successfully concluded the initial development of its promising rotary valve concept for internal combustion engines and was actively seeking avenues for further technological advancement. US patent was issued to Arthur E. Bishop in 1989 [66]. Rather than pursuing opportunities within the automotive industry, Bishop opted for Formula One to leverage the inherent advantages of the rotary valve. Subsequently, a successful public demonstration of their technology was carried out. Figure 21 shows the diagram of the Bishop rotary valve.

Figure 21: Bishop Rotary Valve

In the latter part of 2000, consecutive tests with the poppet valve single-cylinder engine showcased a notable 10% power advantage and enhanced durability. Following this success, the initial V10 engines incorporating this technology were constructed and subjected to thorough testing in 2002. Subsequently, in 2003, an entirely new V10 engine was conceptualized and manufactured. [67]

The Bishop Rotary Valve is a rotating axial flow valve that combines both the inlet and exhaust ports within a single valve. Positioned perpendicularly to the crankshaft axis, there is one valve per cylinder. The steel valve is supported by two shell-type needle roller bearings, ensuring the valve's stepped center portion consistently maintains a slight radial clearance to the housing. The outer diameter of the valve's center portion and the bearings are comparable, facilitating the accommodation of the valve assembly in a seamless bore.

The gas sealing system comprises two axial seals and two circumferential seals positioned near the window, housed within slots in the cylinder head, and preloaded against the outer edge of the valve. These seals operate in a manner akin to piston rings.

Thorough back-to-back testing revealed that both poppet and rotary valve engines exhibit the same peak volumetric efficiency. Despite the rotary valve engine demonstrating breathing capacity comparable to the top performing F1 poppet valve engines, it holds a significant advantage by avoiding the substantial reduction in lifespan commonly associated with F1 poppet valve heads. The absence of inertia-induced loads in the valve train of the rotary valve eliminates the forces responsible for damaging poppet valve heads. The sole durability factor affected by engine speed is the peripheral speed of the sealing elements and bearings. [67]

Rotating at half the engine speed, the valve mitigates the inertia-induced forces that have historically posed challenges in the evolution of reciprocating poppet valve mechanisms since the inception of the internal combustion engine. This particular attribute has motivated numerous inventors over the past century to venture into the development of rotary valve engines. However, these endeavors have typically encountered setbacks, often stemming from issues related to gas sealing, oil sealing, excessive friction, and the susceptibility to thermal and mechanical distortion leading to valve seizure.

4.2.2 Vaztec Rotary Valve

According to Vaztec, it is preferable to characterize it as a simple shaft with a slot cut across its axis, providing a designated flow path. The slot aligns with the port during valve rotation, facilitating gas exchange. Analogous to the conventional poppet valve

train, the rotation of the Vaztec valve is synchronized with the crankshaft to initiate appropriate valve timing events [68]. Darrick Vaseleniuck and David Vaseleniuck of Vaztec, LLC, were granted multiple patents related to the rotary valve design, valve chamber, and valve seal in 2011 and 2015 [69-73]. Figure 22 illustrates the exposed dual-port rotary valve integrated with its cylinder head, as prototyped by Vaztec.

Benefiting from its port design, the Vaztec rotary valve can achieve a remarkably high discharge coefficient when fully open. Vaztec claims significantly superior performance, even when compared to the most advanced poppet valves, resulting in more efficient gas exchange across all engine speeds. The incorporation of the rotary valve, which eliminates a substantial portion of reciprocating motions, has been validated through third-party instrumentation and analysis. This substantiation demonstrates that the Vaztec engine exhibits reduced vibration, with sound pressure measuring only one-third that of the conventional poppet valve engine.

In contrast to many inventors, Vaztec has actively pursued the commercialization of their rotary valve, establishing a facility in North Carolina and making notable strides in the industry. Their latest research indicates a forthcoming pursuit of higher compression ratios and enhancements in the surface-to-volume ratio of the combustion chamber.[68] Currently, Vaztec is collaborating with engine manufacturers to expand the integration of their technology into power sports and, ultimately, automotive production applications, including hybrid systems.

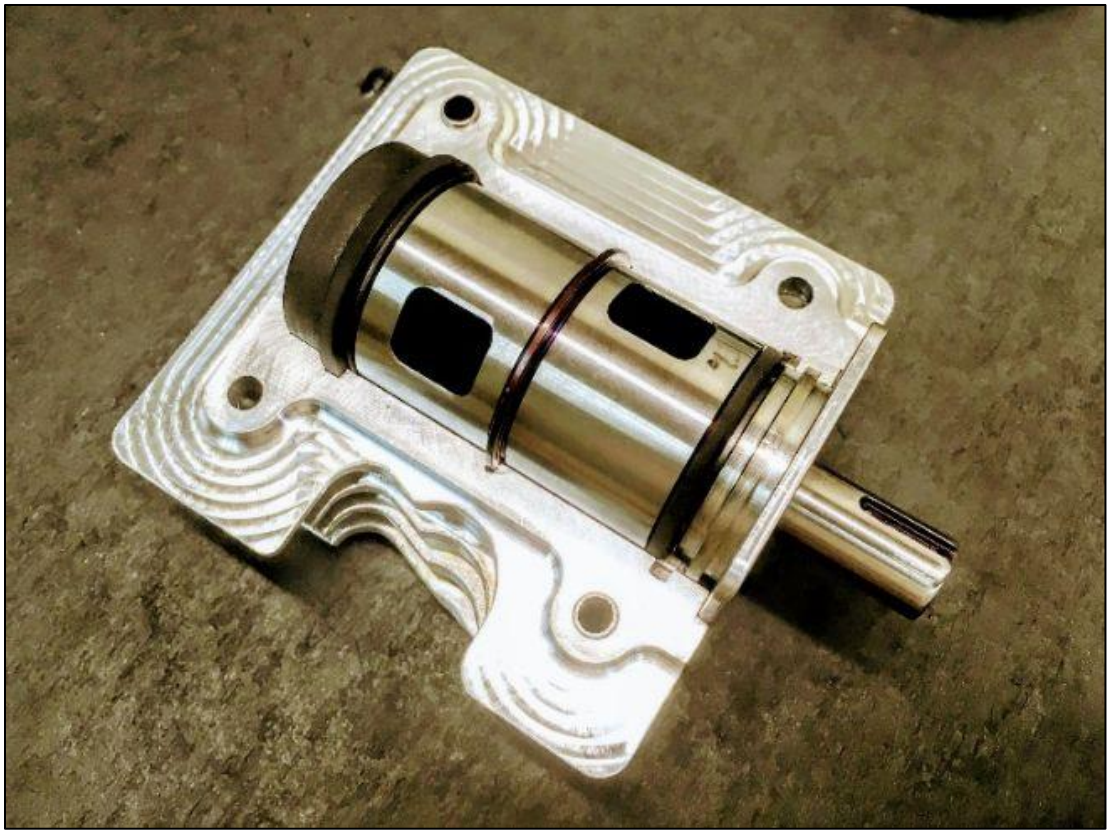

Figure 22: Vaztec Rotary Valve

4.2.3 Coates Rotary Valve

Dating back to the early 1980s, inventor George J. Coates embarked on his journey to develop the Coates rotary valve, making significant contributions in the early 1990s [74]. Patents associated with the spherical rotary valve assembly, valve seal, and spherical valve were granted in 1990 and 1991. Additionally, George J. Coates obtained a patent related to the rotary valve cooling system in 2001 [75].

Similar to Vaztec rotary valve, Coates rotary valve is also installed transversely and can be ultimately identified as a shaft with port cut across its axis. However, distinct from the conventional cylindrical shaped simple shaft, the Coates rotary valve features a

spherical contact and sealing surface. Figure 23 shows Coates rotary valve spherical surface.

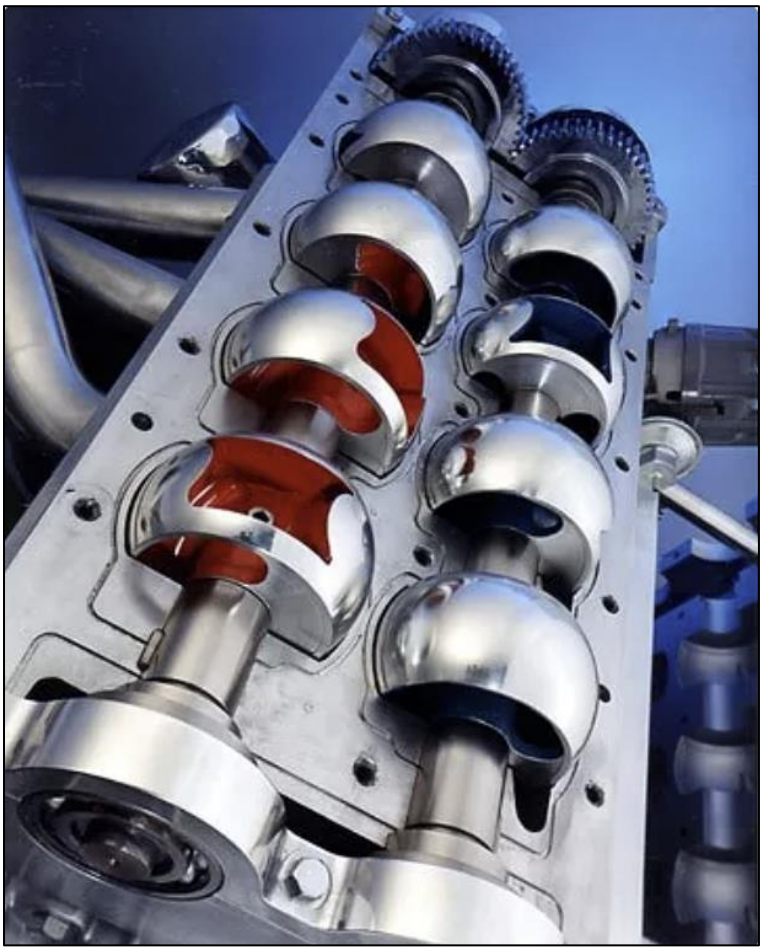

Figure 23: Coates Rotary Valve

The Coates Spherical Rotary Valve System serves as a substitute for conventional poppet valves and their associated components, encompassing springs, valve guides, valve seats, retainers, cotters, pushrods, cam followers, camshaft, camshaft bearings, and various other parts, even including the oil system. The valve system comprises only two moving shafts, eliminating the need for oil-fed bearings or oil spray. As per Coates, the CSRV engine head operates without the necessity of engine oil presence. The absence of

engine oil contact with hot engine components ensures a prolonged durability of the atomic structure of the engine oil. To achieve such a result, the Coates rotary valves rotate on ceramic carbon bearing with no oil lubrication. The spherical surface maintains no contact with any part of the housing. The seals, of a floating type, are crafted from ceramic material. These seals incorporate two piston rings, positioned within a small cylinder-type chamber. Activated by the compression and combustion strokes of the engine, these rings ensure 100 percent sealing effectiveness when compressed. Figure 24 shows the cross section of the Coates rotary valve assembly and the bearings.

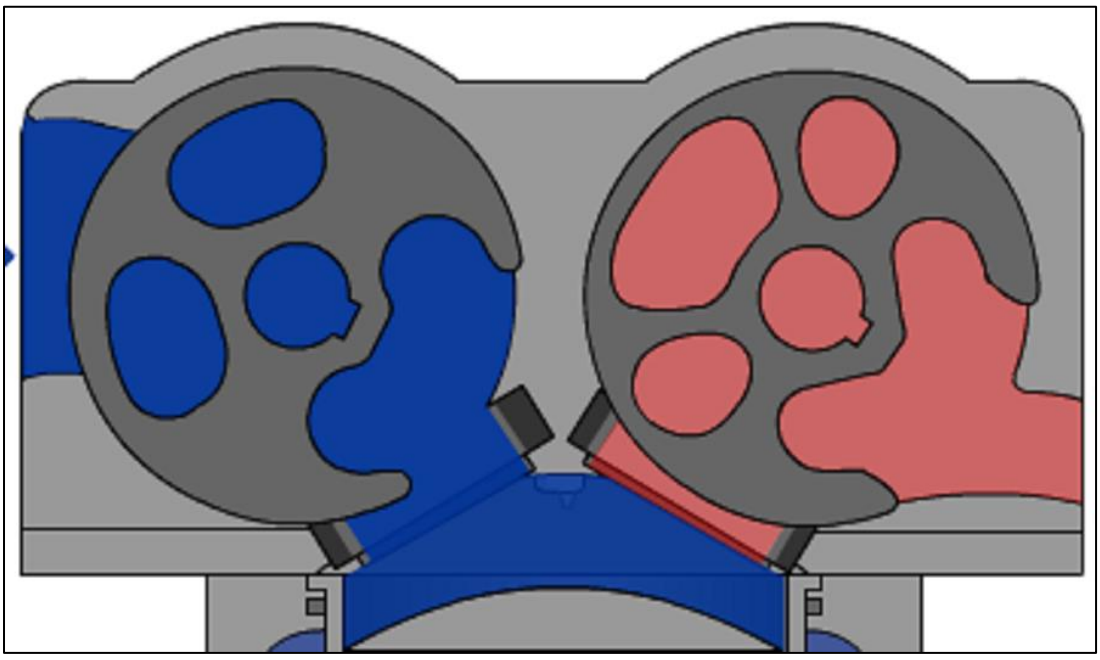

Figure 24: Coates Rotary Valve Cross Section

The continual rotation of the rotary valve serves to dissipate the excess heat accumulated on the valve body during combustion. In contrast to the conventional poppet valve, which remains exposed within the combustion chamber, the rotary valve eliminates the hot spot generated by combustion in the subsequent stroke. This facilitates

the incorporation of higher compression ratios in the design of a combustion engine, leading to enhanced thermal efficiency. Consequently, the engine achieves a more thorough combustion, utilizing a greater proportion of the energy contained in the fuel.

Coates International conducted a series of comparative tests and analyses, demonstrating the advantages of the rotary valve engine, particularly in terms of emission reduction.

4.2.4 Swinging Valve (SwV)

SwV was created and named by Kovács's team. The valve is considered as a type of rotary valve despite its name. The valve is cylindrical shaped with a large offset cutout in the side. The valve is positioned horizontally and rotates in place. The uniqueness is that instead of spinning continuously, SwV rotates back and forth to open and close the port. Each cylinder is assigned two valves to operate intake and exhaust respectively. Figure 25 presents the layout of Swinging Valve.[76]

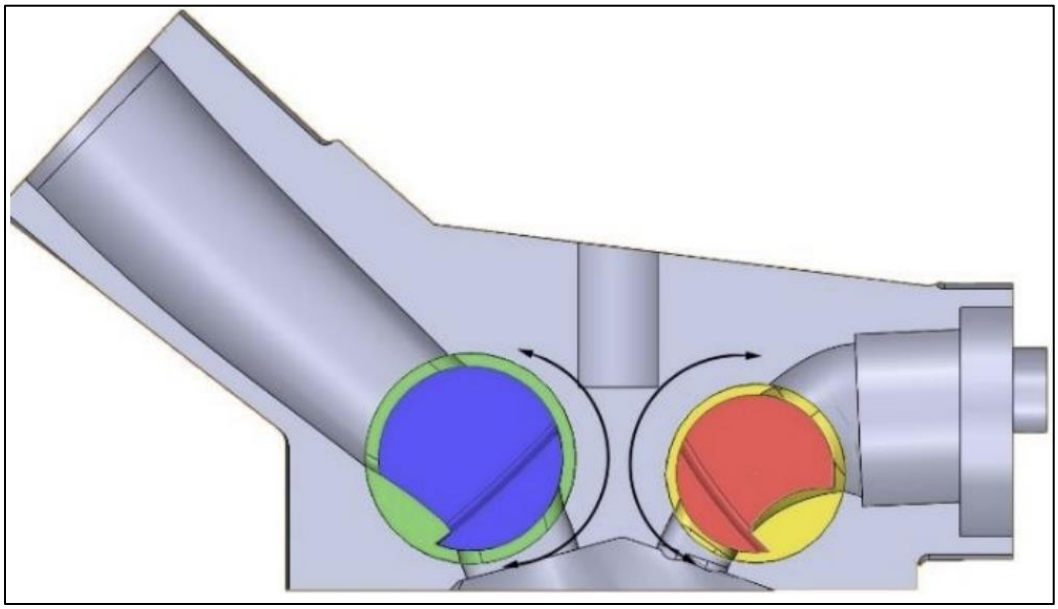

Figure 25: Swinging Valve

4.2.5 Hofmann Valve

Proposed by Hofmann-Drehschiebermotoren in 2012, Hofmann valve was fully developed and manufactured. The valve is shaped into two linked spheres with each sphere functions as a valve. Each sphere has a unique shaped through cutout in the side functions as the valve port opening. The valve is driven by conventional timing chain or timing belt and operate under a fixed timing. According to the inventor, Hofmann valve offers possibility for 20-50% less package and 20-60% less weight on the cylinder head. The rotary valve scavenging areas are equal if not superior to modern poppet valve cylinder head. The unique design does not create excess combustion chamber volume, thus the engine can reach higher compression ratio. With the combustion hotspot rotating away from the combustion chamber, it is less risky to pre-ignition during compression stroke. Figure 27 shows the cross section of Hofmann valve engine. Figure 27 presents the actual manufactured Hofmann valve.[77]

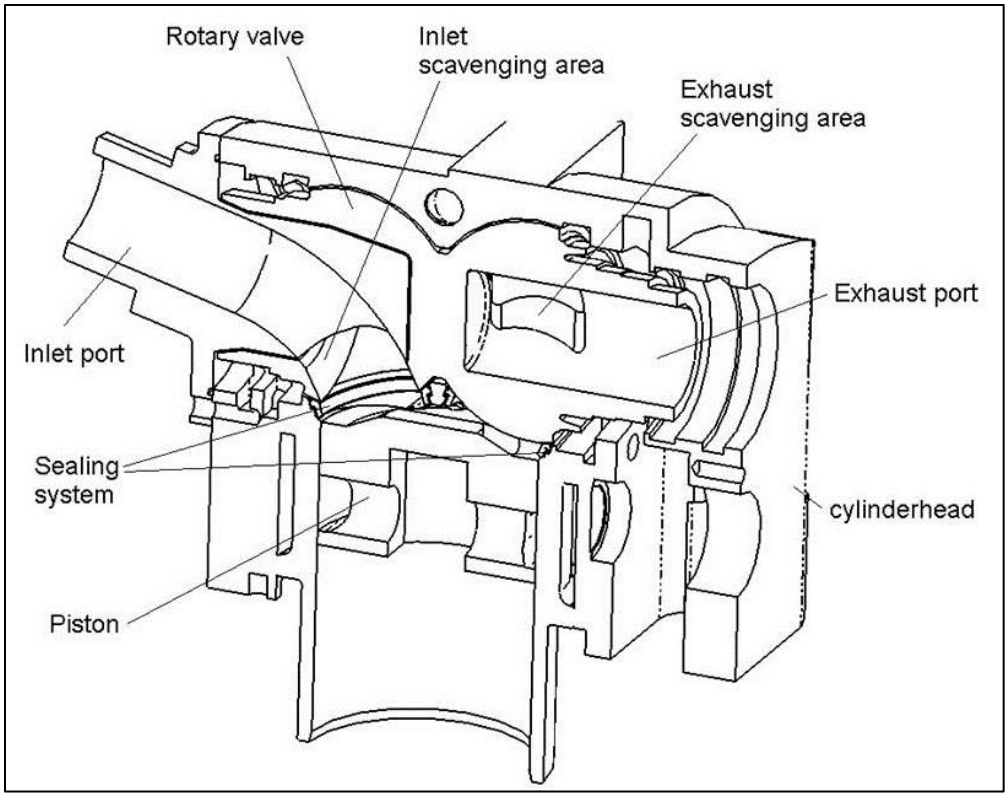

Figure 26: Hofmann Rotary Valve

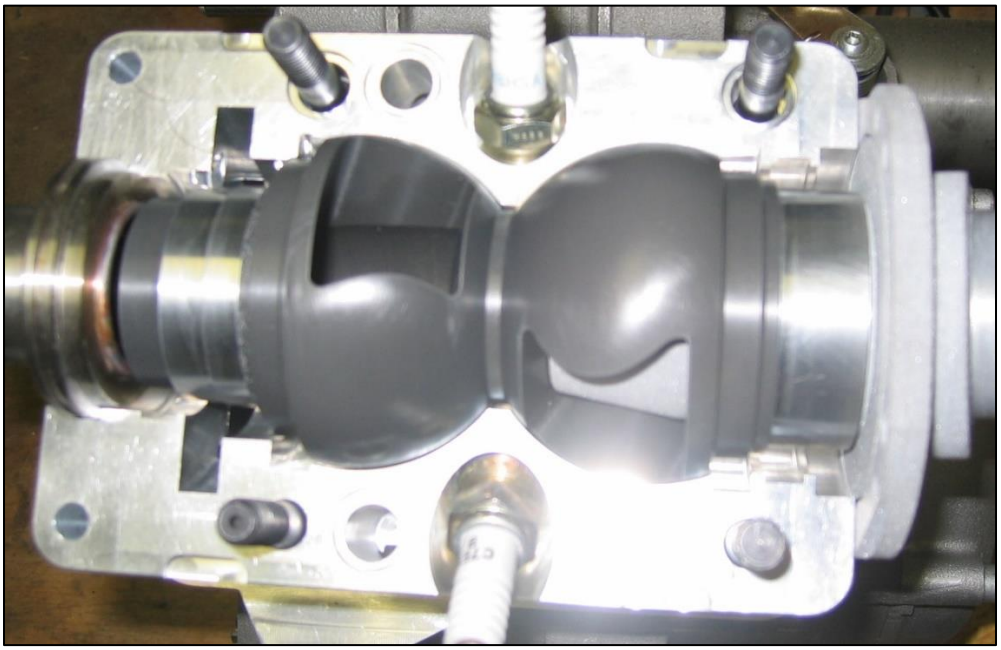

Figure 27: Hofmann Rotary Valve Prototype

4.2.6 Camcon Auto

While the previously mentioned systems feature well-designed structures incorporating innovative rotary valves, none of them have the capability to independently control each cylinder. In simpler terms, all the valves remain interconnected through a virtual camshaft. Developed by Camcon Auto and referred to as Intelligent Valve Actuation (IVA), this system eliminates the need for any camshaft and employs a rotary actuator to drive each individual valve. Each valve is equipped with its own IVA actuator, and these IVA rotary actuators are subject to continuous, rapid feedback control. This allows for the instantaneous adjustment of valve timing, period, or lift at the push of a button. [78]

IVA enables the attainment of both conventional and unconventional event profiles, rendering traditional camshafts obsolete. Valve positions can be continuously monitored during the event through a specialized sensor. According to Camcon Auto's demonstration, IVA can execute a full cycle of valve events or perform a half valve event and revert. This flexibility allows IVA to adapt valve lift, timing, and duration more freely, contributing to emission control under varying working conditions.

However, it's crucial to note that fundamentally, IVA still operates on a conventional poppet valve, inheriting the disadvantages associated with poppet valves. Despite this, Camcon Auto asserts the integration of a built-in fail-safe and automatic protection to prevent the selection of events that pose a risk of valve clash. Figure 28 illustrates a layout featuring multi-cylinder IVA. [79]

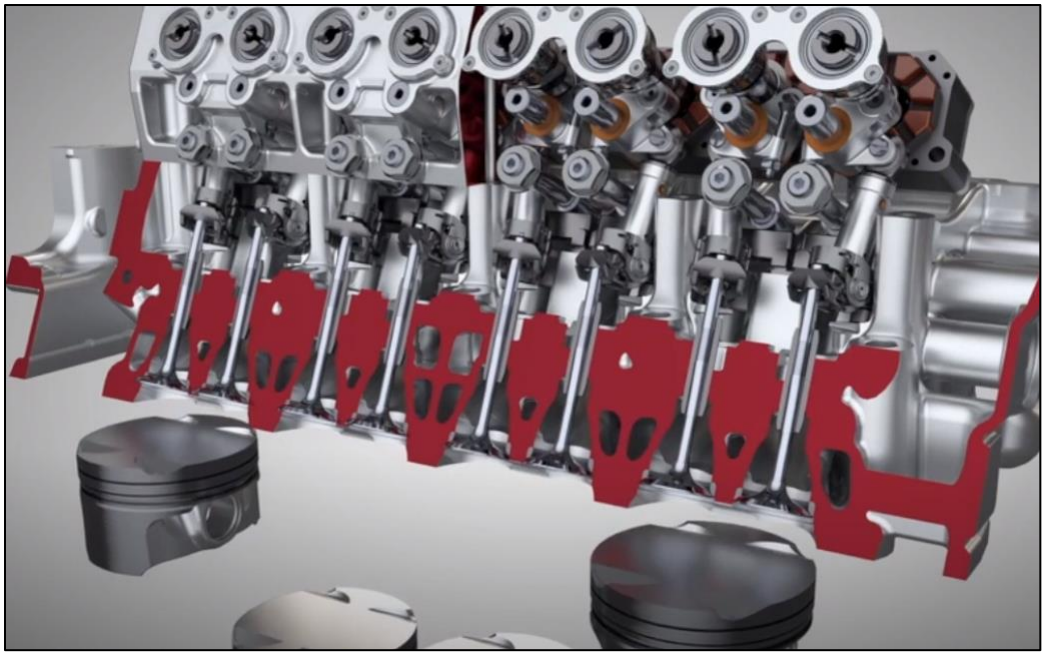

Figure 28: Camcon Auto IVA

4.3 Features and comparison

From the above literature review, rotary valve history and recent works analysis, a few key features are summarized to present the advantages of the rotary valve. The following table 1 is created to list the most recent and developed rotary valves. One can clearly identify the key features and make comparison. Notably, despite not being a typical rotary valve configuration, IVA from Camcon Auto also utilize a servo motor driven rotary actuation mechanism, thus included in the table.

At the very end of the table, a new proposed rotary valve concept carrying more desirable features is expressed.

Table 5: Rotary Valve Feature Comparison

Name	Valves per cylinder	Ports per cylinder	Valve shape	Timing	Lift	Duration	Sealing method	Entry and exit	Driving mechanism	Compression ratio
Bishop Valve	1	1	Cylindrical	Fixed	Fixed	Fixed	Valve surface seal	Axial center port	Timing gear set	High
Vaztec Valve	1	2	Cylindrical	Fixed	Fixed	Fixed	Natural mechanical	Radial through	Timing belt/chain	High
Coates Valve	2	2	Spherical	Fixed	Fixed	Fixed	Valve surface seal	Axial offset port	Timing belt/chain	High
Deng' s Double	2	2	Cylindrical	Fixed	Fixed	Fixed	Valve surface seal	Radial offset cut-	Timing belt/chain	High
Swinging Valve	2	2	Cylindrical	Fixed	Fixed	Fixed	Valve surface seal	Radial offset cut-	Unknown	High
Hofmann Valve	1	2	Spherical	Fixed	Fixed	Fixed	Natural mechanical	Radial through	Timing belt/chain	High
Camcon Auto IVA	2	2	Poppet valve	Variable	Variable	Variable	Natural mechanical	Poppet valve port	Servo motor	High
New rotary	2	2	Bell shape	Variable	Variable	Variable	Natural mechanical	Radial surface	Servo motor	Low
Improved proposed	2	2	Spherical	Variable	Variable	Variable	Natural mechanical	Radial through	Servo motor	High

4.4 Design improvement

The bell-shape rotary valve proposed in this research carries the most preferred features compared to the new concept. However, the inner bell-shape halo space in the valve body creates excess combustion chamber volume when both intake and exhaust valves are closed. Since compression ratio is defined as the ratio of the volume of the cylinder and its head space (including the pre-combustion chamber, if present) when the piston is at the bottom of its stroke (BDC) to the volume of the head space when the piston is at the top of its travel (TDC), the excess combustion chamber volume affects maximum designed compression ratio. In certain engine designs, such as diesel engines or compression-ignition gasoline engines, a compression ratio that is not sufficiently high becomes unacceptable. Figure 29 shows the inner space of the bell-shape rotary valve.

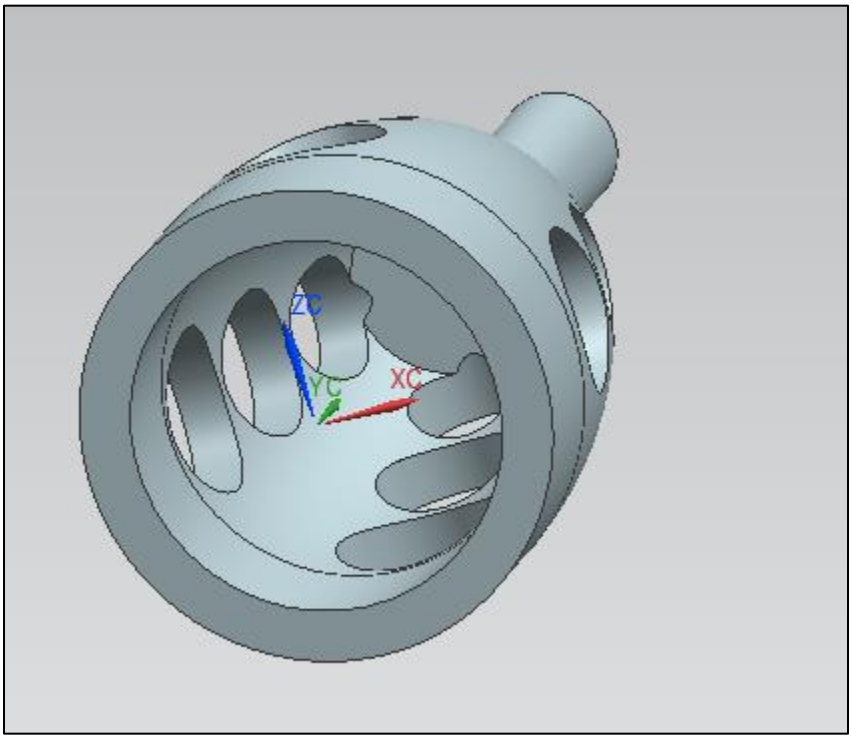

Figure 29: Bell Shape Rotary Valve Inner Space

Moreover, the proposed bell-shape rotary valve includes a valve body and a valve housing which is designed to be press-fitted into the corresponding cylinder head. Since most of the reviewed rotary valve configurations do not include a valve housing, the valve housing is considered as an extra component and the installation procedure is deemed unnecessary.

The outer surface curve of the bell-shape valve body and the inner surface curve of the bell-shape valve housing remain in constant contact and can be classified as a sliding pair. Although the surface curve is created by a section of the circle, it is still possible that the valve body and the valve housing experience seizure under certain conditions.

Ideally, the newly proposed concept preserves two independent rotary valves operating two separate ports for intake and exhaust respectively. In order to save the variable valve capability, the new proposed design is driven by servo motors. The entry and exit ports in the rotary valve are more preferred to be radial through ports, thus the valve can form a natural mechanical seal when it is closed during the combustion stroke. The sliding pair between the valve body surface and the outer surface demands low friction and a lower risk of seizure. A spherical-shape valve body provides more even and larger contact surface and can prevent axial movement thus is more desirable. In order to create a high compression ratio, the valve port interface cannot be too far from the combustion chamber. Excess volumes should be minimized to reduce the compression volume.

Referencing the above requirements, a new horizontally positioned, servo-motor-driven, spherical rotary valve configuration is generated for further evaluation. Figure 30

shows the cross-section of the new rotary valve layout. In the new design, each valve is driven by its electric servo motor rotating around its center axis. When the spindle-shape radial through cut-out is aligned to the opening in the cylinder head, the port is opened. Turning the valve by 45 degrees, the solid section of the valve body is aligned to the opening in the cylinder head to close the port.

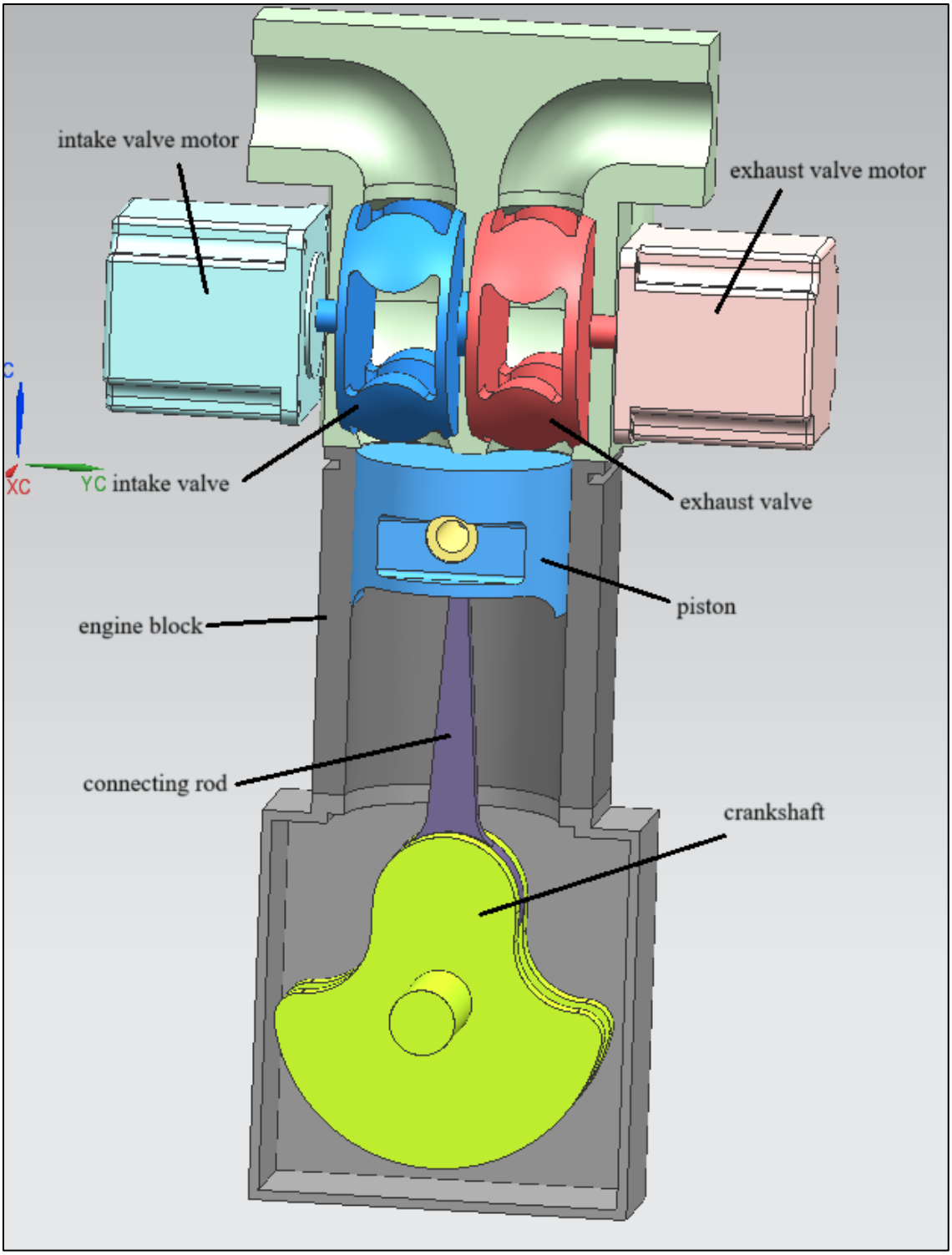

Figure 30: Cross Section of the New Improved Rotary Valve Layout

4.5 Valve related calculation and validation

One of the greatest advantages of the rotary valve is that the valve can create its maximum opening area much quicker than the conventional poppet valve. Instead of a circle through cut-out, the port in the new valve is further improved and features a spindle-shaped cut-out to maximize the valve efficiency. Figure 31 shows the comparison of the initial opening area between the round port and the spindle-shape port.

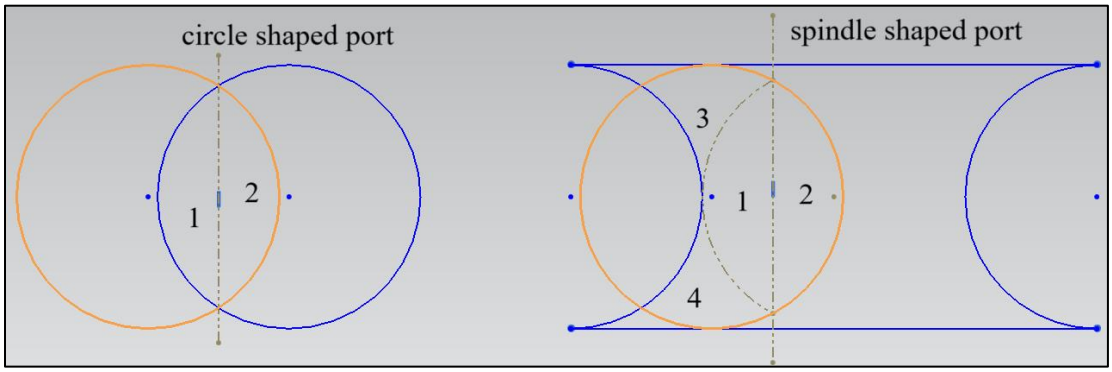

Figure 31: Comparison of the Valve Opening Between Circle and Spindle Port

As seen in Figure 31, the circle valve port opening area can be calculated by the sum of area 1 and area 2, while the spindle shape valve port opening area is assembled by the sum of area 1, area 2, area 3 and area 4, mimicking a moon shape. In other words, with the same critical port diameter and valve rotating speed, the spindle-shaped port will create an opening area faster than the circle port, contributing more air-fuel mass flowing through the port.

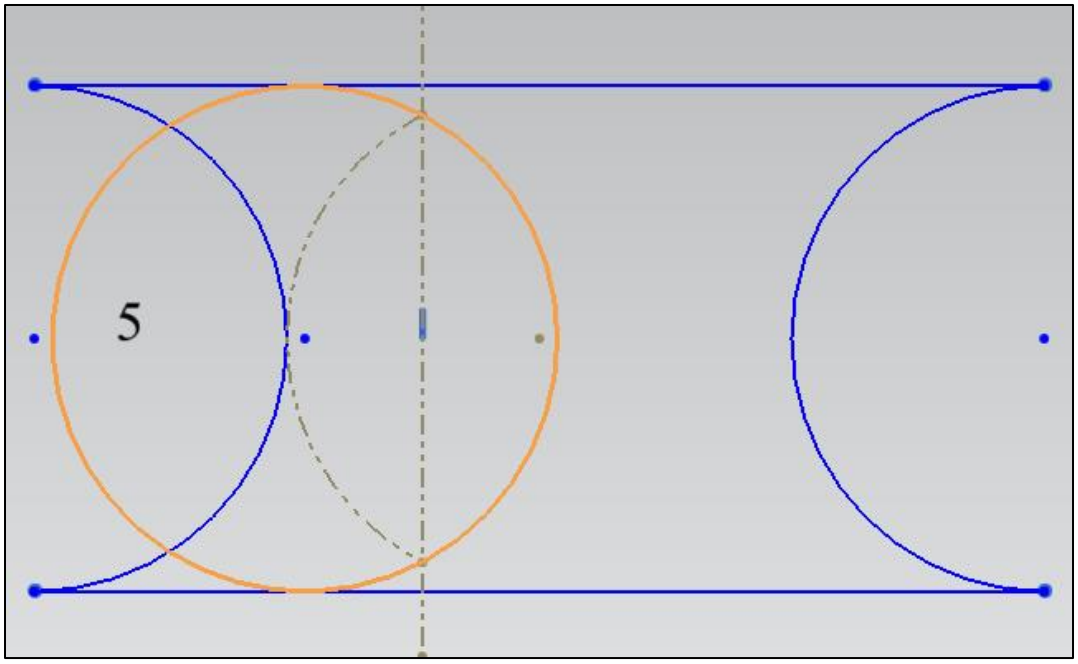

Figure 32: Simplified Spindle Port Problem

Figure 32 is then created to simplify the problem. The valve opening area can be calculated by subtracting the unopened area 5 from the maximum valve opening area.

$$A_5 = \arccos\left\{\frac{r-(r-d_o)}{r}r^2 - \left(\sqrt{r^2-(r-(\mathrm{r}-d_o))^2}(r-(r-d_o))\right)\right\} \qquad (18)$$

The problem can then be solved by the following equation.

$$A_{moon} = \pi r^2 - 2 * A_5 \qquad (19)$$

4.6 Engine geometrical modeling

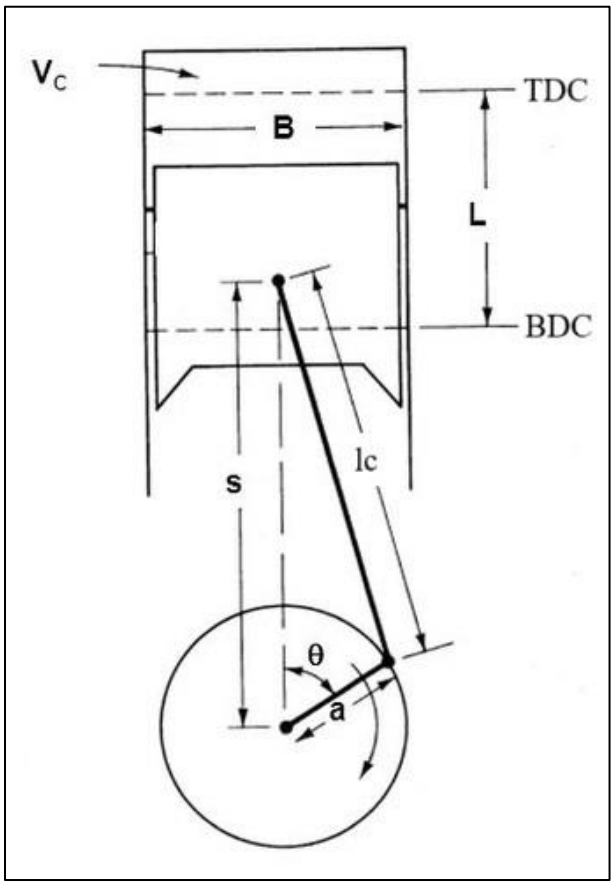

Figure 33: Internal Combustion Engine Geometry

The major geometrical parameters for a reciprocating internal combustion engine are highlighted in Figure 33 and described in the introduction section fundamental principles and benchmark engine model. It is still worth mentioning that the unitary cylinder displacement is the volume displaced by the piston traveling from BDC to TDC thus the total cylinder volume is the sum of displacement volume and clearance volume. The modeling parameters are expressed in the following.

Cylinder bore:

$$B \tag{20}$$

Piston stroke:

$$S \tag{21}$$

The swept volume is usually named as displacement volume:

$$V_d = \pi * S * \left(\frac{B}{2}\right)^3 \tag{22}$$

Clearance volume is calculated from the displacement volume and the stated compression ratio:

$$V_c = \frac{V_d}{r_c - 1} \tag{23}$$

While the actual compression ratio is more important in the computation, it is defined by the ratio between the actual cylinder volume and the clearance volume:

$$r_{ct} = \frac{V_d + V_c}{V_c} \tag{24}$$

The cylinder volume equation can be defined from analyzing the cylinder geometrical parameters.

$$\frac{dV}{d\theta} = \frac{V_d}{2}\left[1 + \frac{L_c}{a} - cos\theta - \sqrt{\left(\frac{L_c}{a}\right)^2 - sin^2\theta}\right] \tag{25}$$

Where,

θ is crankshaft angle,

L_c is connecting rod length,

a is crank throw radius.

4.7 Engine thermodynamic modeling

In the realm of internal combustion engines, the Otto cycle stands as a fundamental framework for understanding the thermodynamic processes that drives spark-ignition engines, commonly employed in gasoline-powered vehicles. Developed by Nikolaus Otto in 1867, this theoretical cycle delineates the engine's operation through four distinct phases: isentropic compression, constant volume heat addition, isentropic expansion, and constant volume heat rejection. As an idealized representation, the Otto cycle serves as a cornerstone for engine simulation studies, providing insights into theoretical performance and efficiency. By comprehensively exploring the cyclic interplay between compression, combustion, expansion, and exhaust processes, researchers can gain valuable insights into the intricate dynamics of internal combustion engines and optimize their designs for enhanced performance and reduced environmental impact. Referencing a typical Otto cycle curve in Figure 34, the four processes are expressed as the following.

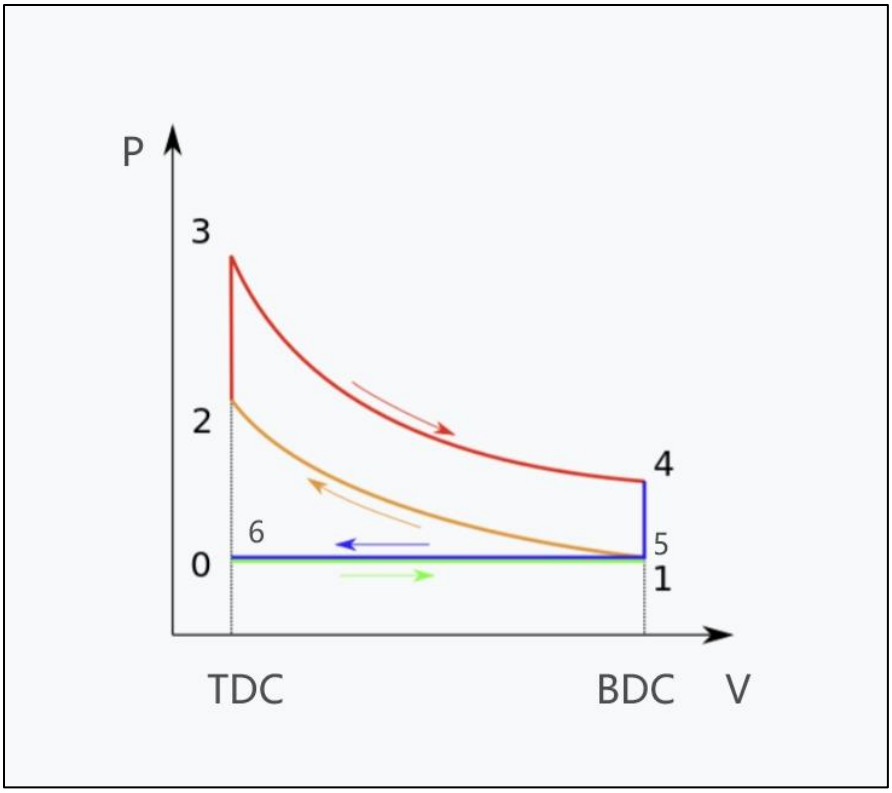

Figure 34: Typical Otto Cycle Curve

Process 1-2: Isentropic Compression

This process represents the compression stroke in the Otto cycle.

The air-fuel mixture is compressed adiabatically (without heat exchange with the surroundings) by the upward movement of the piston.

The compression process is isentropic, meaning it occurs with constant entropy.

As the volume decreases, the pressure and temperature of the air-fuel mixture increase.

$$P_1 = P_6 = P_0 \tag{26}$$

$$V_1 = V_t = V_d + V_c \tag{27}$$

$$T_1 = T_0 \tag{28}$$

$$w_{61} = (V_1 - V_6)P_0 \tag{29}$$

$$m_m = \frac{P_1 V_1}{T_1 R} \tag{30}$$

Where,

V_t represent total cylinder volume,

w_{61} defines the intake work,

m_m defines the mass of fluid inside the cylinder,

R represents universal real gas constant.

The intake temperature T_1 is assumed to have a small enough change than the surround temperature T_0.

Process 2-3: Constant Volume Heat Addition

This process corresponds to the combustion or power stroke in the Otto cycle.

After the compression, a spark plug ignites the compressed air-fuel mixture, leading to rapid combustion.

The combustion process occurs at constant volume, which is an idealized assumption for the spark-ignition engines.

The heat released during combustion increases the pressure and temperature of the gas.

$$P_2 = P_1(r_{ct})^{\gamma} \tag{31}$$

$$V_2 = V_c \tag{32}$$

$$T_2 = T_1(r_c)^{\gamma - 1} \tag{33}$$

$$w_{12} = c_v(T_1 - T_2) \tag{34}$$

$$V_3 = V_C \tag{35}$$

$$Q_{23} = Q_{in} = m_f Q_{HV} \eta_{comb} = m_m c_p (T_3 - T_2) \tag{36}$$

$$P_3 = \left(\frac{T_3}{T_2}\right) P_2 \tag{37}$$

Where,

c_v is the specific heat at constant volume,

γ is the ratio of specific heat,

m_f is the mass of fuel,

m_a is the mass of air,

Q_{HV} is the heat value of fuel,

η_{comb} is the combustion efficiency,

Process 3-4: Isentropic Expansion

This process represents the expansion stroke in the Otto cycle.

The high-pressure, high-temperature gas undergoes adiabatic expansion as the piston moves downward.

Similar to the compression process, the expansion process is isentropic, with a decrease in pressure and temperature as the volume increases.

$$P_4 = P_3 \left(\frac{1}{r_c}\right)^{\gamma} \tag{38}$$

$$V_4 = V_t \tag{39}$$

$$T_4 = T_3 \left(\frac{1}{r_c}\right)^{\gamma - 1} \tag{40}$$

$$w_{34} = c_v (T_3 - T_4) \tag{41}$$

Process 4-5: Constant Volume Heat Rejection

This process corresponds to the exhaust stroke in the Otto cycle.

The exhaust valve opens, and the burned gases are expelled from the cylinder.

Heat is rejected from the system at constant volume, representing the idealized assumption that the exhaust gases are expelled without further expansion.

As the exhaust gases are removed, the pressure and temperature of the remaining gas decrease.

$$P_5 = P_0 \tag{42}$$

$$V_5 = V_1 \tag{43}$$

$$T_5 = T_0 \tag{44}$$

The net indicated work represents the total power produced within the cylinder over one cycle during the expansion stroke, driven by the gas pressure pushing the piston downwards. It is determined through the thermodynamic cycle of the engine, factoring in the losses attributed to heat transfer across the control volume. With all thermodynamic states defined, the indicated work is derivable as the disparity between the work produced in the power stroke and that expended during the compression stroke. The indicated power is consequently characterized as a function of crankshaft revolution and the number of revolutions per power stroke. In this investigation, the engine under consideration operates on a four-stroke cycle, thus the number of revolutions per power stroke is 2.

$$W_{ni} = w_{34} - w_{12} \tag{45}$$

$$W_i = W_{ni}\left(\frac{N}{n}\right) \tag{46}$$

Where,

W_{ni} is net indicated power,

W_i is indicated power.

The thermal efficiency is related to compression ratio.

$$\eta_t = 1 - \left(\frac{1}{r_c}\right)^{\gamma-1} \tag{47}$$

Brake power represents the power effectively delivered by the engine, accounting for mechanical losses incurred during operation. It encompasses the inefficiencies inherent in the engine's mechanical system. The relationship between brake power and indicated power is mediated by mechanical efficiency, a factor heavily contingent upon the design of the engine.

$$\eta_m = \frac{W_b}{W_i} \tag{48}$$

From an approach done by Pulkrabek in 2004, an equation extracted from graphical curve fitting appropriately describe the mechanical efficiency. [1]

$$\eta_m = -0.061\overline{U}_p{}^2 - 1.441\overline{U}_p + 92.62 \tag{49}$$

$$\overline{U}_p = 2 * \mathrm{S} * \mathrm{N} \tag{50}$$

$$\mathrm{bsfc} = \frac{m_f}{W_b} \tag{51}$$

$$\tau = \frac{W_b}{2\pi N} \tag{52}$$

$$\mathrm{bmep} = \frac{W_b n}{V_d N} \tag{53}$$

Where,

$\overline{U}_p$ is average piston speed,

τ is torque,

bsfc is brake specific fuel consumption,

bmep is brake mean effective pressure.

The more flowing into the cylinder means more fuel can be converted into work. To increase the flow, volumetric efficiency is the one to be optimized.

The total mass aspirated into the cylinder is defined as the integral of mass flow rate, for the intake valve, from valve opening to valve closing.

$$M_{as} = \int_{VO}^{VC} dm_r \tag{54}$$

Where,

M_{as} is total mass aspirated,

VO stands for valve opening,

VC stands for valve closing,

m_r is mass flow rate.

The volumetric efficiency is suggested as a function mass flow rate.

$$\eta_v = \frac{\mathrm{M}}{\rho_I V_d} \tag{55}$$

Where,

M stands for inducted mass,

ρ_i stands for intake density,

V_d stands for the displacement volume.

The mass flow rate equation is described as the following.

$$\frac{\mathrm{dM}}{\mathrm{dt}} = \rho_u A_f c_u \sqrt{\left[\frac{2}{\gamma - 1}\right]\left[\left(\frac{P_d}{P_u}\right)^{\frac{2}{\gamma}} - \left(\frac{P_d}{P_u}\right)^{\frac{\gamma+1}{\gamma}}\right]} \tag{56}$$

Where,

A_f is the effective valve opening area,

c is the speed of sound,

P_d is the downstream pressure,

P_u is upstream pressure,

ρ_u is upstream density.

It is worth mentioning that the upstream condition and the downstream condition are relative. For the intake valve, the in cylinder space is the downstream while for the exhaust valve, the in cylinder space is the upstream.

Under the condition where the difference between upstream pressure and downstream pressure is too great, a sonic velocity chock flow can occur. The chock flow condition is described as the following ratio.

$$\frac{P_u}{P_d} = \left(\frac{\gamma + 1}{2}\right)^{\frac{\gamma}{\gamma-1}} \tag{57}$$

The mass flow rate under chocked flow condition is expressed as the following equation.

$$\frac{\mathrm{dM}}{\mathrm{dt}} = \rho_u A_f c_u \left(\frac{2}{\gamma + 1}\right)^{\frac{\gamma+1}{2(\gamma-1)}} \tag{58}$$

The flow coefficient is needed to define the effective valve opening area.

$$A_f = C_f A_c \tag{59}$$

Where,

C_f is flow coefficient,

A_c is the actual valve opening area.

4.7.1 Flow coefficient prediction

Unlike the bell-shaped rotary valve discussed above that can be simplified and treated as "orifice, corner taps", the new spherical rotary valve imitates a "full port ball valve". An approximation is applied to the experimental data of the ball valve flow coefficient found in the table from MyDatabook.[80] Since the new spherical rotary valve design has an intake valve opening port of 28mm and an exhaust valve opening port of 26mm, the size difference is considered minimal and can be neglected. Figure 35 shows the approximation curve for 6-degree polynomial approximation. The fitted flow coefficient equation is expressed as the following.

$$C_f = -1.389 * 10^{-9}x^6 + 2.353 * 10^{-7}x^5 - 1.225 * 10^{-5}x^4 + 0.0003316x^3 - 0.002754x^2 + 0.2592x + 0.07972 \tag{60}$$

Where,

x is the valve position angle.

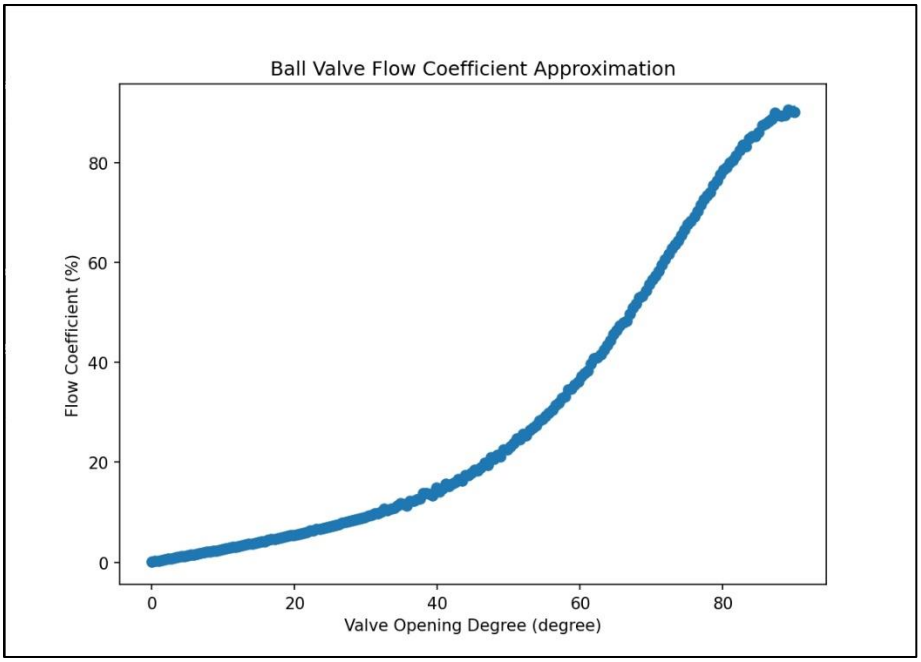

Figure 35: Ball Valve Flow Coefficient Approximation Curve 6-Degree

The data obtained from the database is the flow coefficient at each opening degree angle of a full port ball valve and the dataset is linearly organized. Cross-validation divides the dataset into k folds and uses k-1 folds to perform the prediction and then test the outcome with the leftover test fold. Doing so, breaks the consistency of the linear dataset. In this study, random sampling approach is attempted to protect dataset consistency. Instead of dividing the dataset into k folds, the random sampling takes 20% of data from random indices to form the test set while leaving the 80% remaining to be fitting set. Figure 36 shows an example of cross-validation on 6-degree approximation.

The cross-validation runs 10 times with each group testing data passing into the outcome for validation. Table 6 and Table 7 show the result.

Table 6: 5-Degree Polynomial Approximation Cross-Validation Result

No. of run	Mean squared error (MSE)	Average MSE	MSE standard deviation	MSE standard error	95% confidence interval
1	0.1038	1.3485	1.3919	0.4402	1.3485±0.8627
2	0.0824				
3	3.6728				
4	2.2184				
5	0.2620				
6	0.1553				
7	0.7025				
8	3.2886				
9	0.2281				
10	2.7706				

Table 7: 6-Degree Polynomial Approximation Cross-Validation Result

No. of run	Mean squared error (MSE)	Average MSE	MSE standard deviation	MSE standard error	95% confidence interval
1	0.4385	0.1914	0.2532	0.0800	0.1914±0.1570
2	0.0703				
3	0.0690				
4	0.0373				
5	0.8555				
6	0.0790				
7	0.0429				
8	0.0568				
9	0.2470				
10	0.0176				

The k-fold cross validation for the 6-degree polynomial resulted in a mean MSE of 0. 1914+/- 0. 1507 the 95% confidence interval was calculated using the standard error of the mean. 6-degree approximation result is selected for future evaluation.

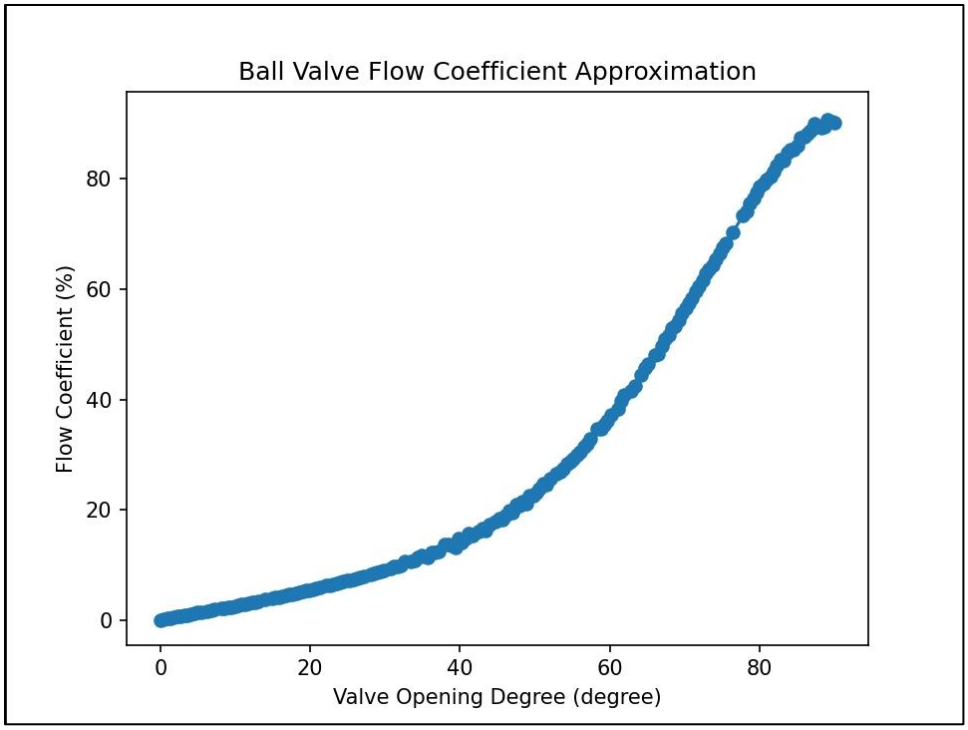

Figure 36: Ball Valve Flow Coefficient Approximation Cross-Validation 6-Degree

During the process of intake and exhaust, the open system equation is used to determine the cylinder properties. Figure 37 shows the diagram of an open system.

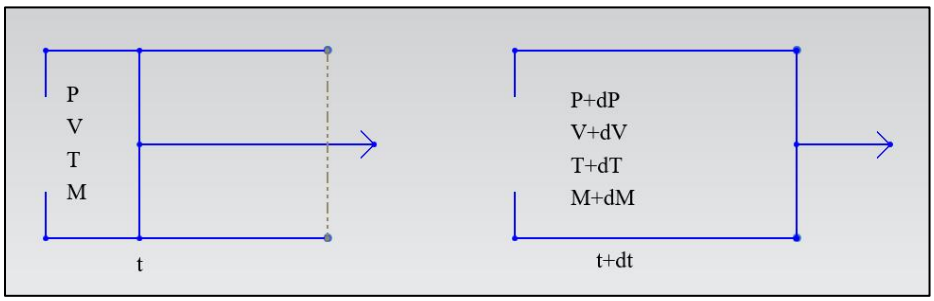

Figure 37: Gas Open System Diagram

The heat transfer during the intake process is assumed to be small enough to be neglected. For the inward flow, the energy equation of the internal energy difference of the cylinder contents between two states can be expressed as the following.

$$\mathrm{dE} = \mathrm{dH} - \mathrm{PdV} \tag{61}$$

$$\mathrm{dE} = C_v d(MT) \tag{62}$$

The energy of the mass flows into the cylinder is defined as the following.

$$\mathrm{dH} = C_p T_a d\mathrm{M} \tag{63}$$

Where,

T_a is air temperature,

C_p is the specific heat for gas in constant pressure process,

C_v is the specific heat for gas in constant volume process,

Combine equation 61, 62, 63 and replace the cylinder mass and temperature variation with pressure and volume variation, the equation in the following can be assembled.

$$C_v d\left(\frac{PV}{R_s}\right) = C_p T_a dM - PdV \tag{64}$$

Where,

R_s is the mass specific gas constant of the cylinder contents.

The constant pressure specific heat is related to the constant volume value by

$$C_p = C_v + R \tag{65}$$

The ratio of the specific heats is

$$\gamma = \frac{C_p}{C_v} \tag{66}$$

Where, for air

C_v is 20.8,

γ is 1.4.

Equation 64 can then be reformed as the following,

$$\mathrm{VdP} + \frac{R_s}{20.8}\mathrm{PdV} = R_s \gamma T_a dM \tag{67}$$

Equation 56 and 58 can be converted to crankshaft position angle related as the following.

For the normal mass flow:

$$\frac{\mathrm{dM}}{\mathrm{d\theta}} = \frac{\rho_u A_f c_u}{\omega}\sqrt{\frac{2}{\gamma - 1}\left[\left(\frac{P_d}{P_u}\right)^{\frac{2}{\gamma}} - \left(\frac{P_d}{P_u}\right)^{\frac{\gamma+1}{\gamma}}\right]} \tag{68}$$

For the chocked flow:

$$\frac{\mathrm{dM}}{\mathrm{d\theta}} = \frac{\rho_u A_f c_u}{\omega}\left(\frac{2}{\gamma - 1}\right)^{\frac{\gamma+1}{2(\gamma-1)}} \tag{69}$$

Where,

ω is engine angular velocity.

Four cases can occur during the engine gas exchange process. They are normal inward flow, normal outward flow, choked inward flow and choked outward flow.

In this study, the simulation is built upon the standard Otto cycle, thus valve overlapping condition is not considered. For the intake process, the final energy equation is assembled as following.

$$\frac{\mathrm{dP}}{\mathrm{d\theta}} = -\frac{R_s \gamma P}{V}\frac{dV}{d\theta} + \frac{R_s \gamma C_1}{V}\frac{dM_i}{d\theta} \tag{70}$$

Where,

$C_1 = T_i$ in this case, we assume $T_i = T_a$ the atmosphere temperature,

P is the initial pressure, in this case, the pressure at the beginning of the intake stroke is P_a, the atmosphere pressure,

V is the initial volume, in this case, v_c the clearance volume,

$\frac{dV}{d\theta}$ is replaced by equation 25.

4.8 Result and discussion

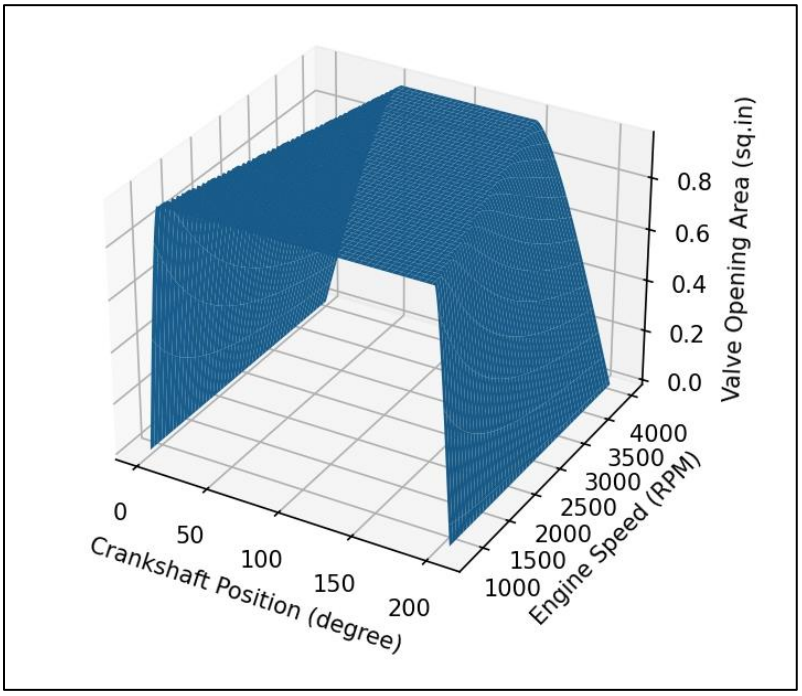

Figure 38: Spherical Rotary Valve Opening Area 3D Plot

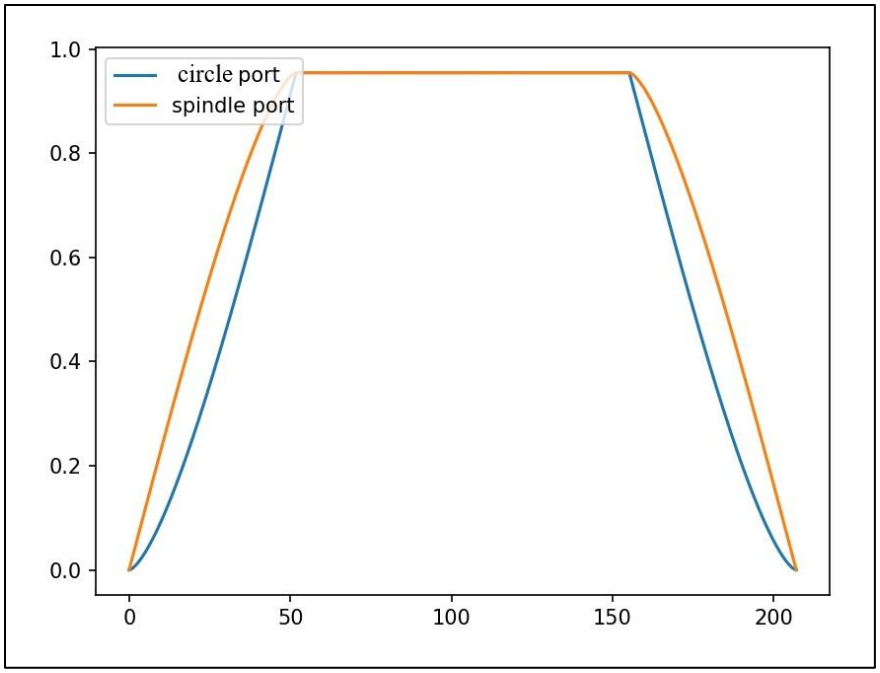

Figure 39: Valve Opening Area Comparison Between Spindle and Circle Port Under 4000 RPM

Figure 38 shows the 3D plot of the valve opening area calculation for the spherical-shaped rotary valve with spindle-shaped valve port. The maximum valve opening area reaches up to 0.954 sq.in. which is bigger than the previous vertical bell rotary valve's 0.795 sq.in by 20% and it may not be obvious for lower engine speed working conditions. However, while the engine runs faster, one can easily identify that the spindle-shaped port gains valve opening area much more aggressively compared to the circle-shaped port. Up to 3% more volumetric efficiency gain is calculated during the valve opening process benefiting from the spindle-shape port. Figure 39 shows the valve opening area curve comparison between the spindle-shaped port and circle-shaped port under 4000 rpm. Although the maximum valve opening area remains the same for both port designs, one can easily point out that the spindle-shaped valve port opens more

harshly and creates a larger opening area at any point before the completion of the maximum opening area. Correspondingly, the spindle-shaped port gains volumetric efficiency much quicker too.

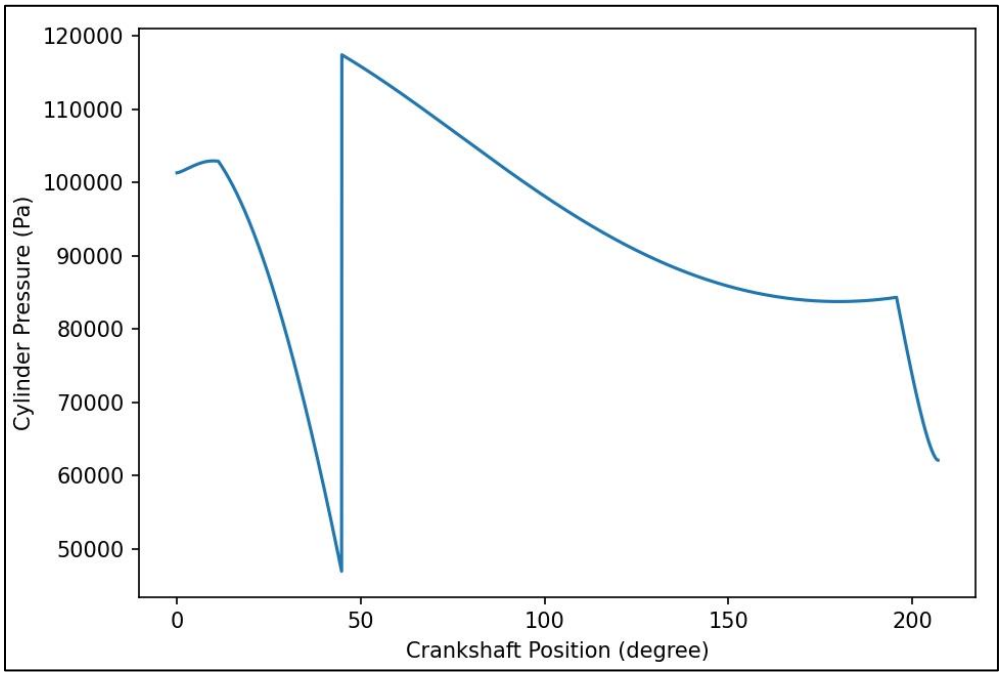

Figure 40: Cylinder Pressure Curve During Intake Process Under 2500 RPM

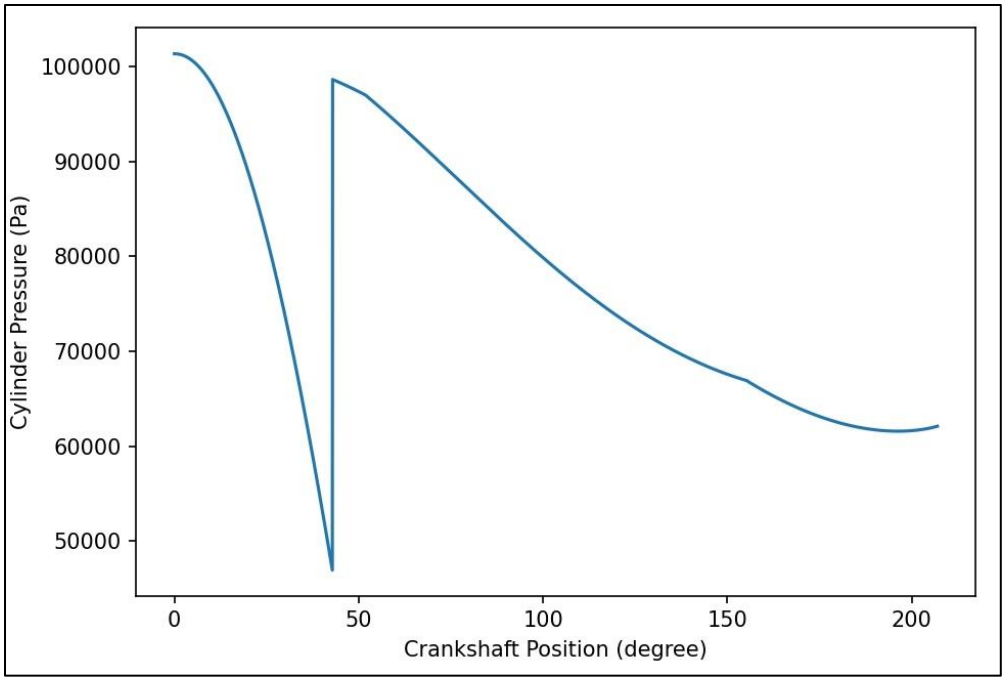

Figure 41: Cylinder Pressure Curve During Intake Process Under 4000 RPM

Figure 40 and Figure 41 show the cylinder pressure curve during the intake process under 2500 rpm and 4000 rpm. Differing from the conventional poppet valve which causes the cylinder pressure to drop drastically and recover in the late stage of intake stroke, the improved rotary valve generates a unique curve due to its motion property. At the beginning of the intake process, the piston departs from TDC and the rotary valve starts to open. At this moment, the valve opening area is small enough to generate higher vacuum in the cylinder causing choked flow and the cylinder pressure decreases quickly. Soon after, as the piston moves down, the rotary valve gains valve opening area aggressively and balances the intake pressure and the cylinder pressure. Choked flow stops, the flow property becomes normal and the cylinder pressure increases to a much higher level. With the piston moving past half of the stroke, the piston velocity reaches its maximum. Although the rotary valve is fully open, due to higher piston speed,

the cylinder pressure sees some losses. Then, in the final stage of the intake stroke, the valve starts to close, the piston slows down as it is approaching BDC and the cylinder pressure experiences another decrease. It is also obvious that under a lower engine speed, the cylinder pressure change is smaller, which shows consistency compared to reality.

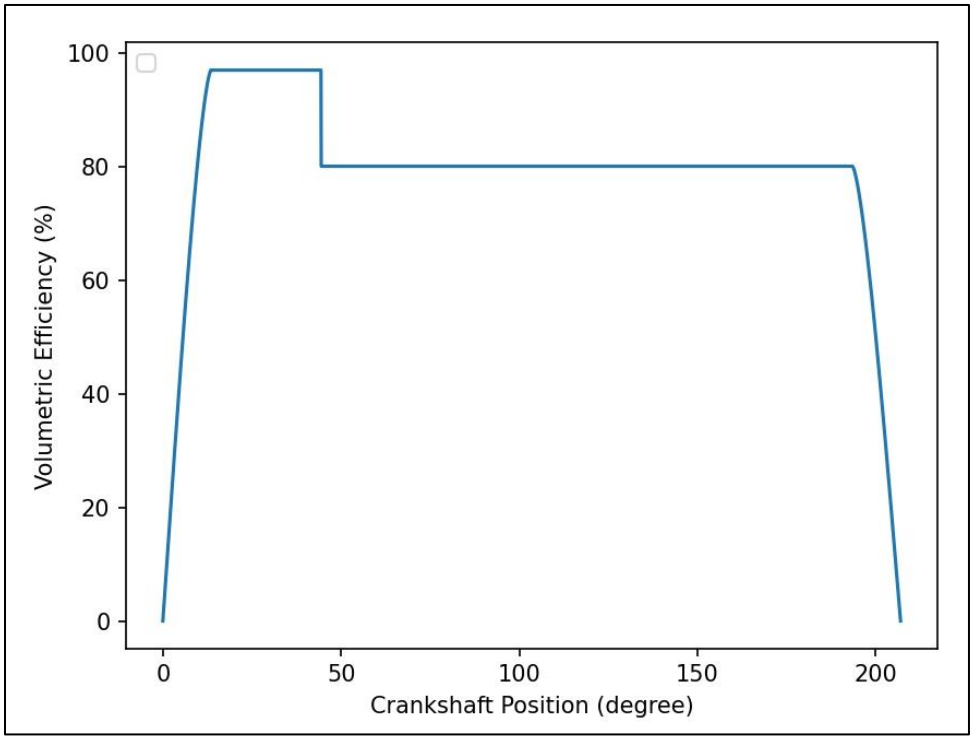

Figure 42: Volumetric Efficiency for The Spindle Shaped Port at 2500 RPM

Figure 42 shows the volumetric efficiency for the spindle-shaped port at 2500 rpm. Unlike the conventional poppet valve, which struggles during choked flow processes, the improved rotary valve can achieve greater efficiency by capitalizing on its rapid opening motion. By maintaining the valve position angle, the improved rotary valve enables the volumetric efficiency to remain at its maximum for a significantly extended duration compared to conventional valves.

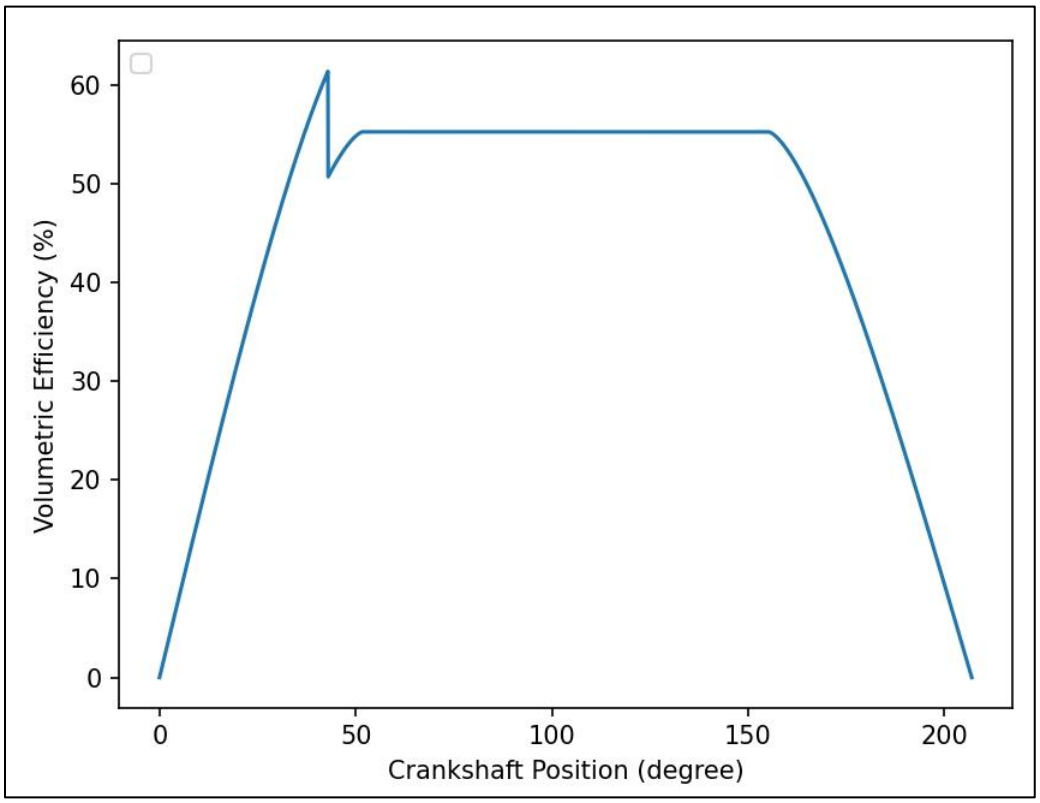

Figure 43: Volumetric Efficiency for The Spindle Shaped Port at 4000 RPM

Figure 43 shows the volumetric efficiency of the improved valve at 4000 rpm. With higher engine speed, the maximum efficiency valve position duration is shorter. The maximum volumetric efficiency also decreases as expected.

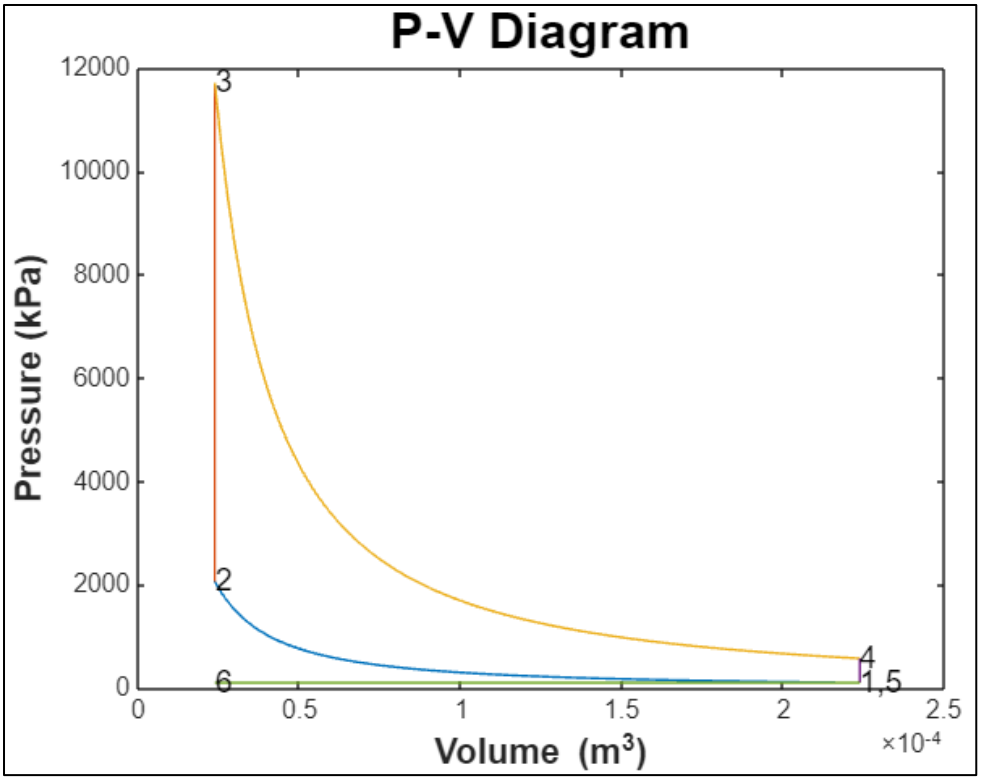

Figure 44: P-V Diagram of the Engine Under 4000 RPM

Figure 44 shows the P-V diagram of the engine while running under 4000 rpm. The simulated engine model carries over the parameters from the benchmark engine which is a single-cylinder engine with only 200cc of displacement. Contributed by the rotary valve being able to stay in the maximum volumetric efficiency for a much longer period, the intake stroke negative work is minimal, as indicated by process 6-1 in the figure. Calculation shows 0.54354 or 54.354% thermal efficiency.

4.9 Conclusions

The proposed new engine design with the proposed improved spherical rotary valve is deemed feasible and performed better than conventional poppet valve. The design simplified the construction of the engine cylinder head and optimized the rotary valve body shape and port shape.

The novel spindle-shaped port is validated to perform better than the conventional circle port with up to 3% volumetric efficiency gain during the valve opening process. The maximum valve opening area created by the new spherical rotary valve is 0.954 sq.in. which is 20% larger than the previous bell-shape rotary valve's 0.795 sq.in. The valve flow coefficient prediction successfully described the spherical rotary valve flow property.

In this research, predictions are made regarding in-cylinder pressure and volumetric efficiency, both of which can be explained using engine kinematics and mechanical principles. The resulting P-V diagram from the engine simulation provides brief evidence that the rapid opening feature of the new rotary valve greatly reduces negative work.

CHAPTER 5 CONCLUSIONS AND FUTURE WORKS

5.1 Conclusions

The study went through numerous research papers, textbooks, webpages and news. The fundamentals of the internal combustion engine, valve technology, modern engine technology, rotary valve history and the current works were thoroughly reviewed. These studies have laid a robust foundation and made significant contributions to research in internal combustion engine related research.

This work demonstrated the first vertical rotary valve concept and the result showed brief evidence of the advantages and feasibility of the application. The vertical rotary valve was found to be more efficient than conventional poppet valve when running below 4400 RPM. While the construction of the vertical rotary valve may not have been flawless, its outcomes remain significant contributions to the ever-evolving field of engine valve research.

Considering both the strengths and weaknesses of the vertical rotary valve, an even more refined transverse rotary valve was developed. This advanced design not only streamlined the engine cylinder head but also optimized flow dynamics. By introducing a new spindle-shaped port and a revolutionary spherical valve body, the enhanced design achieved a remarkable 20% increase in maximum valve opening area and realized up to a 3% enhancement in volumetric efficiency during the valve opening process.

5.2 Future works

Experimental valve flow coefficient. Engine valve flow coefficients serve not only to characterize valve/port designs' performance but also to model gas exchange in 0D/1D engine simulations. Typically, these coefficients are estimated under small pressure ratios and ambient air conditions. However, during engine operation, the pressure ratio, pressure, and temperature levels span a much wider range. In this work, the rotary valve is simplified into a "full port ball valve" which resembles the reality. The experimental data was selected and polynomial approximation method was applied to predict the valve flow coefficient which was then cross-validated using root mean square error method. During the prediction, a minimal difference of the valve size was neglected. The above-mentioned assumptions benefited the study with relatively simple and accessible resources, however, can be further refined and improved. 3D Computational Fluid Dynamics modeling and simulations can be introduced for better investigation and validation. An actual flow bench test experiment using 3D printed rotary valve can be designed to collect real world experimental data for finer approximation.

Variable valve timing. Similar to Camcon Auto IVA which is also driven by electric servo motor, the proposed rotary valve in this research has the ability to adjust timing, lift and duration, while the term lift here represents valve opening area. With different program, the servo motor could start the valve opening process at any point of crankshaft angle, making the system variable timing. The same process can happen at the valve closing, making it a variable duration system. During a lower engine speed with low load, the servo motor can reverse the valve and start closing before reaching the

maximum valve opening area, resulting in a variable lift system. Simulations and predictions can be undertaken to validate this theory.

REFERENCE

1. Pulkrabek, W.W., *Engineering fundamentals of the internal combustion engine*. 2004.
2. David, J., *Experimental and modeled effects of camshaft manufacturing errors on the dynamics of high speed valve trains.* Department of Mechanical and Aerospace Engineering, 1998: p. 89-92.
3. Kumar, G.A. and C.N. Raj, *Design and Analysis of an IC Engine Piston and Piston Rings by Using Three Different Materials.* International Journal of Advances in Mechanical and Civil Engineering, 2017. **4**.
4. Heywood, J.B., *Internal combustion engine fundamentals*. 2018: McGraw-Hill Education.
5. Davis, M. *The Ultimate Source Guide for Flathead Ford V-8 Performance*. 2023; Available from: https://www.motortrend.com/how-to/flathead-ford-engine-guide/.
6. McKelvie, S. *A Critique of the "Flathead" or Side-Valve Engine Design*. 2012 [cited 2022; Available from: https://stevemckelvie.wordpress.com/2012/07/12/a-critique-of-the-flathead-or-side-valve-engine-design/.
7. Cantt, W. *Combustion chambers*. 2011; Available from: https://pautomotivemechanics.blogspot.com/2011/05/combustion-chambers.html.
8. Writer, S. *Mopar Max Wedge Cylinder Heads Guide - Size Does Matter*. 2006; Available from: https://www.motortrend.com/how-to/mopp-060800-mopar-max-wedge-cylinder-heads/.
9. Kuo, T.-W. and R.D. Reitz, *Computation of premixed-charge combustion in pancake and pent-roof engines.* SAE Transactions, 1989: p. 1239-1257.
10. Mashkour, M.A. and M.H. Ibraheem, *Numerical Simulation of pent-roof combustion chamber in a SI Engine.* Journal of Mechanical Engineering Research and Developments, 2020. **43**(7): p. 422-433.
11. Varol, Y., et al., *CFD modeling of heat transfer and fluid flow inside a pent-roof type combustion chamber using dynamic model.* International Communications in Heat and Mass Transfer, 2010. **37**(9): p. 1366-1375.
12. Wondergem, A.M. and M. Ivantysynova. *The impact of the surface shape of the piston on power losses*. in *Fluid Power Systems Technology*. 2014. American Society of Mechanical Engineers.
13. Le, A.T., et al., *Performance and combustion characteristics of a retrofitted CNG engine under various piston-top shapes and compression ratios.* Energy sources, part A: Recovery, utilization, and environmental effects, 2020: p. 1-17.
14. Magda, M. *Inside Piston Design: Dish, Dome, and Flat Top Pistons Explained*. 2017; Available from: https://www.motortrend.com/features/inside-piston-design-dish-dome-flat-top-pistons-explained/.
15. Deng, B., et al. *Double rotary valve engine design*. in *IOP Conference Series: Earth and Environmental Science*. 2020. IOP Publishing.

16. Gabelish, P.W., A.R. Vial, and P.E. Irving, *Rotary Valves for Small Four-Cycle IC Engines*. 1989, SAE Technical Paper.
17. Cross, R., *Rotary Valves for Internal Combustion Engines.* Proceedings of the Institution of Automobile Engineers, 1935. **30**(1): p. 296-326.
18. Muroki, T., Y. Moriyoshi, and S. Sekizuka, *A study of rotary valve for a single cylinder engine*. 1999, SAE Technical Paper.
19. Horrocks, G.D., *A numerical study of a rotary valve internal combustion engine*. 2001.
20. Robinson, A.C., et al., *A computational fluid dynamics investigation comparing the performance of an alternative valvetrain design against a traditional poppet valvetrain.* ASME Open Journal of Engineering, 2022. **1**.
21. Hunter, M.C.I., *Rotary valve engines, 1946.* London, Hutchinson.
22. Peliks, R.B., *Novel design of a rotary valve using axiomatic design*. 2005, Massachusetts Institute of Technology.
23. UK, C.B.H. *ICONIC ENGINES: ROTARY VALVE NORTON*. Available from: https://www.oldbikemart.co.uk/iconic-engines-rotary-valve-norton/.
24. Self, D. *Rotary-Valve Internal Combustion Engines*. 2004; Available from: http://www.douglas-self.com/MUSEUM/POWER/unusualICeng/RotaryValveIC/RotaryValveIC.htm#asp.
25. JohnWood. *Aspin Rotary Valve Engines*. 2000; Available from: http://www.aspin.info/.
26. Chow, P., H. Watson, and T. Wallis, *Combustion in a high-speed rotary valve spark-ignition engine.* Proceedings of the Institution of Mechanical Engineers, Part D: Journal of Automobile Engineering, 2007. **221**(8): p. 971-990.
27. Boretti, A. and J. Scalzo, *Design of 65 degree V4 Moto GP engines with pneumatic poppet valves or rotary valves*. 2015, SAE Technical Paper.
28. Muzakkir, S., M. Patil, and H. Hirani, *Design of innovative engine valve: Background and need.* International Journal of Scientific Engineering and Technology, 2015. **4**(3): p. 178-181.
29. Brown, T.L., P. Atluri, and J.P. Schmiedeler, *Design of high speed rotary valves for pneumatic applications.* Journal of Mechanical Design, 2014. **136**(1): p. 015001.
30. Zibani, I., J. Chuma, and J. Marumo, *Design, Test and Implementation of a single piston rotary valve Engine Control Unit.* IFAC Proceedings Volumes, 2014. **47**(3): p. 5665-5670.
31. Tsu, T.-c., *Theory of the inlet and exhaust processes of internal-combustion engines*. 1949.
32. Theobald, M.A., B. Lequesne, and R. Henry, *Control of engine load via electromagnetic valve actuators.* SAE transactions, 1994: p. 1323-1334.
33. Stone, R., et al. *Intelligent Valve Actuation–A Radical New Electro-Magnetic Poppet Valve Arrangement*. in *Proceedings of the 26th Aachen Colloquium Automobile and Engine Technology, Germany*. 2017.
34. Myers, E.P., *A Novel Engine Head Design Using a Rotary Valve System in Traditional Four-Stroke Internal Combustion Engines*. 2019: Western Carolina University.
35. Mu, H., et al., *Technical research on improving engine thermal efficiency.* Advances in Mechanical Engineering, 2022. **14**(9): p. 16878132221125032.
36. Kopac, M. and L. Kokturk, *Determination of optimum speed of an internal combustion engine by exergy analysis.* International Journal of Exergy, 2005. **2**(1): p. 40-54.
37. Wang, Y., *Introduction to engine valvetrains*. 2006: SAE international.

38. Dong, W., *Design and fabrication of erect rotary valve for internal combustion engine*. 2016, Middle Tennessee State University.
39. Trzesniowski, M., *Rennwagentechnik: Grundlagen, Konstruktion, Komponenten, Systeme*. 2014: Springer-Verlag.
40. Calabretta, M., D. Cacciatore, and P. Carden, *Valvetrain friction-modeling, analysis and measurement of a high performance engine valvetrain system.* SAE International Journal of Engines, 2010. **3**(2): p. 72-84.
41. Youd, J. *Understanding valve spring sience and selection, for optimization, performance and longevity*. 2011.
42. Roodink, T., *Literature review on stabilizing high speed valve-and drivetrain concepts for racing applications.* 2016.
43. *engine timing diagram*.
44. x-engineer.org. *How to Calculate the Volumetric Efficiency of an Internal Combustion Engine*. 2019; Available from: https://x-engineer.org/automotive-engineering/internal-combustion-engines/performance/calculate-volumetric-efficiency/.
45. Yin, S., *Volumetric efficiency modeling of a four stroke IC engine*. 2017, Colorado State University.
46. x-engineer. *Volumetric efficiency of an internal combustion engine*. 2023; Available from: https://x-engineer.org/calculate-volumetric-efficiency/.
47. Haq, Z. *Volumetric Efficiency of Engines*. 2023; Available from: http://zahurul.buet.ac.bd/ME417/ME417_VolumetricEfficiency.pdf.
48. Meyer, J., *Engine modeling of an internal combustion engine with twin independent cam phasing*. 2007, The Ohio State University.
49. Giampaolo, T., *Compressor handbook: principles and practice*. 2023: CRC Press.
50. Padeanu, A. *VW Group Not Abandoning ICE, Puts Skoda In Charge Of Small Engine Development*. 2023 [cited 2024; Available from: https://www.motor1.com/news/662705/skoda-developing-ea211-engine/.
51. HOGAN, M. *Volkswagen Will Also Stop Developing Internal Combustion Engines*. 2021 [cited 2024; Available from: https://www.roadandtrack.com/news/a35901171/volkswagen-will-also-stop-developing-internal-combustion-engines/.
52. Waldersee, V. *Mercedes-Benz delays electrification goal, beefs up combustion engine line-up*. 2024 [cited 2024 Jan. 08]; Available from: https://www.reuters.com/business/autos-transportation/mercedes-benz-hits-cars-returns-forecast-inflation-supply-chain-costs-bite-2024-02-22/.
53. Ewing, J. *Mercedes-Benz will shift its focus to electric vehicles by 2025*. 2021 [cited 2024; Available from: https://www.nytimes.com/2021/07/22/business/mercedes-benz-electric-vehicles.html.
54. Pandolfo, C. *Mercedes-Benz delays EV goals because of weak demand, will continue to build gas-powered cars*. 2024 [cited 2024; Available from: https://www.foxbusiness.com/fox-news-auto/mercedes-benz-delays-ev-goals-weak-demand-continue-gas-powered-cars.
55. Rosevear, J. *Ford will postpone about $12 billion in EV investment as buyers become more cautious*. 2023 [cited 2024 Jan. 08]; Available from: https://www.cnbc.com/2023/10/26/ford-will-postpone-about-12-billion-in-ev-investment.html.

56. Peter Valdes-Dapena, C.I. *Ford is cutting back F-150 Lightning electric truck production*. 2024 [cited 2024 Jan. 08]; Available from: https://www.cnn.com/2024/01/19/business/ford-trimming-ev-pickup-production/index.html.
57. Mason, B., K. Lawes, and K. Hirakawa, *Rotary Valve 4-Stroke Engines for General Purpose Power Equipment and Unmanned Systems.*
58. Deng, B., et al. *Single rotary valve engine design*. in *IOP Conference Series: Earth and Environmental Science*. 2020. IOP Publishing.
59. Behrens, J.W., *Modification and performance evaluation of a mono-valve engine*. 2011: Southern Illinois University at Carbondale.
60. Bari, S., S. Hossain, and I. Saad, *A review on improving airflow characteristics inside the combustion chamber of CI engines to improve the performance with higher viscous biofuels.* Fuel, 2020. **264**: p. 116769.
61. NAKANO, H., *Combustion Chamber Shape Optimization for Small Diesel Engines by Coupling CFD and AI* Mitsubishi Heavy Industries Technical Review, 2023. **60**.
62. Waghmare, M.T.S. and B. Lande, *A Cycle Simulation Model Of A Diesel Engine For Predicting The Performance Using Python.* 2022.
63. Beloiu, D.M., *Modeling and analysis of valve train, part I-conventional systems.* SAE International Journal of Engines, 2010. **3**(1): p. 850-877.
64. Kakaee, A.H., B. Mashadi, and M. Ghajar, *A novel volumetric efficiency model for spark ignition engines equipped with variable valve timing and variable valve lift Part 1: model development.* Proceedings of the Institution of Mechanical Engineers, Part D: Journal of Automobile Engineering, 2017. **231**(2): p. 175-191.
65. *Patents for F01L 7 - Rotary or oscillatory slide-valve gear or valve arrangements (1,661)*. Available from: https://www.google.com/patents/sitemap/en/Sitemap/F01/F01L/F01L_7_15.html.
66. Bishop, A.E., *Rotary valve for internal combustion engines*. 1989.
67. Wallis, T., *The Bishop Rotary Valve*, in *AutoTechnology*. 2007. p. 3.
68. Garrett, N.H., et al., *Development of a Rotary Valve Engine for Handheld Equipment*. 2022, SAE Technical Paper.
69. Darrick Vaseleniuck, D.V., *Seal*. 2015: United States.
70. Darrick Vaseleniuck, D.V., *Rotary valve chamber*. 2015: United States.
71. Darrick VASELENIUCK, D.V., *Head assembly and valve-less internal combustion engine*. 2015: Canada.
72. Darrick Vaseleniuck, D.V., *Seal apparatus for rotary valve engine*. 2015.
73. Darrick Vaseleniuck, D.V., *Rotary valve*. 2015: United States.
74. Coates, G.J. *Reference*. 2024; Available from: http://www.georgejcoates.com/references/.
75. International, C. *Patents*. 2024 [cited 2024; Available from: https://www.coatesengine.com/patents.html.
76. Kovács, L., B. Bolló, and S. Szabó, *A Complex Comparatrive Study of Two Dissimilar Engine Valve Constructions, for the In-Cylinder Flow Behaviour of a High Speed, IC Engine.* Acta Polytechnica Hungarica, 2024. **21**(4).
77. Hofmann-Drehschiebermotoren. *Rotary valve engines, designed by Hofmann-Drehschiebermotoren*. 2017 [cited 2024; Available from: https://www.hofmann-dsm.com/products/rotary-valve/.

78. Auto, C. *Single Cylinder Combustion Development System*. 2018; Available from: https://camcon-automotive.com/wp-content/themes/camcon-auto/documents/Camcon-Single-Cylinder-Conversions.pdf.
79. Auto, C. *iVT basics*. 2018; Available from: https://camcon-automotive.com/the-basics/.
80. MyDatabook. *Flow Coefficient, Opening and Closure Curves of Full Bore Ball Valves*. 2024 [cited 2024; Available from: https://www.mydatabook.org/fluid-mechanics/flow-coefficient-opening-and-closure-curves-of-full-bore-ball-valves/.